THERMAL BEHAVIOUR OF DIELECTRIC MATERIALS DURING RAPID HEATING

by

DAIPAYAN SARKAR

Presented to the Faculty of the Graduate School of

The University of Texas at Arlington in Partial Fulfillment

of the Requirements

for the Degree of

MASTER OF SCIENCE IN MECHANICAL ENGINEERING

THE UNIVERSITY OF TEXAS AT ARLINGTON

May 2012

To my Dad

ACKNOWLEDGEMENTS

I have been fortunate to meet and work with some of the best minds in my area of interest which has been Heat Transfer Physics which has helped me enter the league of researchers. I guess my wish to work under Dr. A. Haji-Sheikh was quite inevitable as he has been a pioneer in heat transfer. His enthusiasm, professionalism and passion for research kept inspiring and motivating me in my work. His boundless experience as an academician made my initial path in research a smooth one. He is always open for new challenges in research and the time I spent under his guidance as a student investigator has helped me fill many voids that I had from my past experience in heat transfer and mathematics. I truly express my gratitude towards you Professor for giving me the greatest opportunity to work with you and become the person I am now.

Next I would like to acknowledge my committee members, Dr. Dereje Agonafer and Dr. Seiichi Nomura for agreeing to be in my defense committee by taking time out of their busy schedule. My appreciations to Ms. Debi Barton for always notifying me about the upcoming deadlines and helping me keep pace with all the required processes. Special thanks to Dr. Albert Tong and Mr. Shubhankar Mitra for their unconditional support and strong belief that I had the potential in me. My sincere acknowledgements to Mr. Saeed Ghalambor and Peter Martinez for supporting me in their valuable time and sharing their experiences Special thanks to people who have known me for a long time, George, Rutu, Diya and Asma. They have been the greatest listeners to an awful speaker as I have jaded them with things related to this research and other stuff. They have never walked away and always helped me relax. Thank you for being so supportive guys.

Finally, my parents and Shreya who have seen me in my best and worst. Every research requires a driving force that takes it all the way till the end. The force in my work has been Shreya. Your support has been immense and explicit. Mom for being such a loving and caring person. I miss the times that we shared back home addressing my problems past dinner, those late night meals before my exams and many more. While writing this thesis I have missed you a lot as I did not have my best friend around me on all those sleepless nights. Dad you have shown me how to fight back in life. It is true that falling down isn't failure but staying down is failure. Words fail to describe my parents' efforts, the sacrifices they made to make me the person who I am. For all the discomfort I have caused to you all, I have tried my best to put in that much amount of determination, dedication, sincerity and hard work behind this thesis. Dad you have always been the source of my success, my spine, a good friend who just has insane amount of patience and belief in me. To you I dedicate this thesis.

April 14, 2012

ABSTRACT

THERMAL BEHAVIOUR OF DIELECTRIC MATERIALS

DURING RAPID HEATING

Daipayan Sarkar, M.S.

The University of Texas at Arlington, 2012

Supervising Professor: Abdolhossein Haji-Sheikh

The objective of this research is to understand the temperature variation in dielectric materials of different geometry. The work is divided into three major segments. The Thermal Wave model has been taken into consideration as the classical Fourier law of heat conduction breaks down when a dielectric material of sub-micron geometry is heated rapidly. The first part of the work discusses primarily about the temperature distribution in a semi-infinite dielectric material, followed by the temperature profile in a finite body (plate) and finally mathematical formulation is presented for a two-layered body. The thermal wave equation is used because in dielectric materials the lag time due to temperature (τ_t) is much less than the lag time due to heat flux (τ_q), $(\tau_t \ll \tau_q)$ and hence all the terms describing the effects of τ_t in the governing equation used for expressing the phenomena of Hyperbolic Heat Conduction in a material can be neglected. Boundary conditions of first and second kind are applied to the thermal wave equation for all three cases that are discussed later in the study. The classical Laplace

Transform method has been used as a tool to analyze the mathematical models for all the illustrations presented in the study. Analytical solutions are obtained for semi-infinite and finite bodies for different boundary conditions and a mathematical formulation has been presented to calculate the heat flux at the interface for a two-layered dielectric body. Due to large complexity of the problem and intense use of algebra several Mathematica subroutines are developed to compute and examine the thermal behavior of dielectric materials during rapid heating.

TABLE OF CONTENTS

LIST OF ILLUSTRATIONS

LIST OF TABLES

NOMENCLATURE

C	Thermal capacitance, ρC_p, ($J/m^3 K$)
C_p	Specific heat of the material, ($J/kg K$)
h	Height of the lattice when phonons are at rest
H	Height of reduced region where phonons are vibrating rapidly
k	Thermal conductivity of the dielectric material, ($W/m K$)
L	Length of the dielectric body, (m)
q	Surface heat flux, (W/m^2)
S	Volumetric heat source, (W/m^3)
t	Time, (s)
t_d	Delay in time, (s)
t_f	Final time or total time, (s)
T	Temperature of the dielectric body, (K)
T_0	Wall temperature of the dielectric material, (K)
T_i	Initial temperature of the body, (K)
x	coordinate, (m)

Greek symbols

α	Thermal diffusivity
η	Dimensionless time
η_d	Delay in Dimensionless time
η_f	Final Dimensionless time
θ	Dimensionless temperature
λ	Dimensionless dummy variable

Greek symbols- continued

ξ	Dimensionless space
ρ	Density, (kg/m^3)
σ	Wave Speed, (m/s)
τ_q	Lag time due to heat flux, (s)
τ_q^*	Dimensionless lag time due to heat flux

CHAPTER 1

INTRODUCTION

1.1 Literature Review

The Boltzmann transport theorem is often modified for evaluating the temperature field during a rapid energy transport in micro-scale devices. An existing mathematical model uses a wave model to describe the variation of temperature fields in dielectric fields.

The classical Fourier heat conduction model considers the heat propagation to be at infinite speed. This model does not adequately describe the temperature field due to phonons transport at very small time within a thin device. Accordingly, Cattaneo [1] and Vernotte [2] modified the Fourier heat conduction model for application to non-metallic bodies where phonons are the major heat carriers. However, the transport of energy by free electrons and phonons contribute to the conduction of heat in metals as reported by Tien and Lienhardt [3]. Later, Qui and Tien [4, 5] used a two-step radiation-heating model to study absorption of photon energy by electrons and subsequent heating of the lattice through electron-phonon coupling. A modified Boltzmann transport theorem [5] leads to the development of linear systems in order to study the transport of energy in microscale devices. Surveys of earlier studies of energy transport in dielectric materials are in Joseph and Preziosi [6], Tzou [7], and Ho et al. [8].

This work presents systematic analytical techniques that can serve as a tool for determination of temperature in thin films in the presence of a thermal wave. First, consideration is given to determination of the temperature solution in semi-infinite bodies using the classical method of Laplace transforms. Investigators have earlier worked on this topic before [17] but the mathematical formulation and analysis has been presented in this work again because we would require the results obtained for the semi-infinite case to validate the results obtained for a plate. The solution obtained is highly accurate. The mathematical derivation of the energy if a material has free electrons, the electrons can be considered separately and, at a given time, *t*, equation presented is based on the hypothesis that electrons and lattice of a substance absorb energy input.The electron gas temperature, $T_e(t)$ is different from the lattice temperature, $T_l(t)$; however, they are related [5, 7] by equation,

$$T_e(t) = T_l(t) + \tau_t \frac{\partial T_l(t)}{\partial t} \tag{1.1}$$

and τ_t is a time delay equal to the ratio of lattice heat capacitance to the electron/lattice coupling coefficient. According to Eq. (1.1), the temperatures of electron gas and lattice are related. The energy balance applied to an elemental volume at location ***r*** and at time t yields the relation,

$$-\nabla \cdot \mathbf{q}(\mathbf{r},t) + S(\mathbf{r},t) = C_e \frac{\partial T_e(\mathbf{r},t)}{\partial t} + C_l \frac{\partial T_l(\mathbf{r},t)}{\partial t} \tag{1.2}$$

The parameter C_e is the volumetric heat capacities of electron gas and C_l is that for the lattice. Assuming thermophysical properties are constant, the substitution of T_e from Eq. (1.1) into Eq. (1.2) yields,

$$-\nabla \cdot \mathbf{q}(\mathbf{r},t) + S(\mathbf{r},t) = = C \frac{\partial T_l}{\partial t} + C\tau_e \frac{\partial^2 T_l(\mathbf{r},t)}{\partial t^2} \tag{1.3}$$

where $C = C_e + C_l$ and the variable $\tau_e = \tau_t C_e / C$ is defined as the thermalization time in [4] and the lag time in [7].

Next, the Fourier equation,

$$\mathbf{q}(\mathbf{r},t) = -k_e \nabla T_f(\mathbf{r},t) \tag{1.4}$$

needs to be modified as to become

$$\mathbf{q}(\mathbf{r},t) + \tau_q \frac{\partial \mathbf{q}(\mathbf{r},t)}{\partial t} = -k\nabla T_l(\mathbf{r},t) - k\tau_t \frac{\partial}{\partial t} \nabla T_l(\mathbf{r},t) \tag{1.5}$$

After eliminating **q** within Eq. (1.3) and Eq. (1.5) and keeping only the second order terms of Taylor series, the final form of the microscale thermal conduction equation is [9]

$$\nabla \cdot [k\nabla T(\mathbf{r},t)] + \tau_t \frac{\partial\{\nabla \cdot [k\nabla T(\mathbf{r},t)]\}}{\partial t} + \left[S(\mathbf{r},t) + \tau_q \frac{\partial S(\mathbf{r},t)}{\partial t} \right] = C\frac{\partial T(\mathbf{r},t)}{\partial t} + C(\tau_e + \tau_q)\frac{\partial^2 T(\mathbf{r},t)}{\partial t^2} \quad (1.6)$$

when $\tau_t \to 0$, this equation reduce to the thermal wave equation,

$$\nabla \cdot [k\nabla T(\mathbf{r},t)] + \left[S(\mathbf{r},t) + \tau_q \frac{\partial S(\mathbf{r},t)}{\partial t} \right] = C\frac{\partial T(\mathbf{r},t)}{\partial t} + C\tau_q \frac{\partial^2 T(\mathbf{r},t)}{\partial t^2} \quad (1.7)$$

where τ_q related to the speed of propagation of thermal wave. As discussed in [7], the parameter τ_q for metals, is the same as τ_F, known as the electron relaxation time at the Fermi surface. As discussed in [4, 5], the parameter $\tau_t = C_l / G_e$ where G_e is the coupling factor between electron gas and the lattice. Further information related to these parameters is in [9-12].

.The wave propagation in finite bodies due to a volumetric heat source is presented in [19]. The investigators have used Green's function solution to compute the temperature. Other investigators have performed experiments in biological materials like processed meat and concluded the existence of a damped wave model [20]. In the past investigators have done experiments on gold films to obtain data of femtosecond laser heating and computed their results using finite difference methods [21]. Recently studies related to wave propagation in multilayer bodies were analyzed by [22, 23]. Most of these works emphasize more on the use of finite difference schemes or Green's function solution. Khadwari et al. have studied the thermal behavior of composite slabs that consisted of two metal layers and adopted the Laplace transform approach to solve the problem [22].

1.2 Research Objectives

The work that is presented here in this thesis emphasizes on the use of classical Laplace transform method. The work has been restricted to the use of boundary conditions of first and second kind to dielectric materials of different geometries which are presented from

Chapter 2-5 in this study. Prior to presentation of the temperature field in a plate by utilizing a Laplace transform technique, a brief discussion of the temperature solution in a semi-infinite body is presented. The solution technique is similar to that in Baumeister and Hamill [17], with some modification. This is necessary since, at small time, the temperature solution in a plate is the same as that for a semi-infinite body with the same surface condition. The Chapter 6 of this study shows the mathematical formulation of a two-layered non-metallic material with perfect contact condition subjected to boundary condition of second kind. Analytical solutions were obtained which gave us a highly accurate temperature solution for all the cases that are discussed later in the text. To make our argument on accuracy even stronger, we have illustrated the difference in error in Figure 1.1. Hence analytical solution will give us a highly accurate temperature solution.

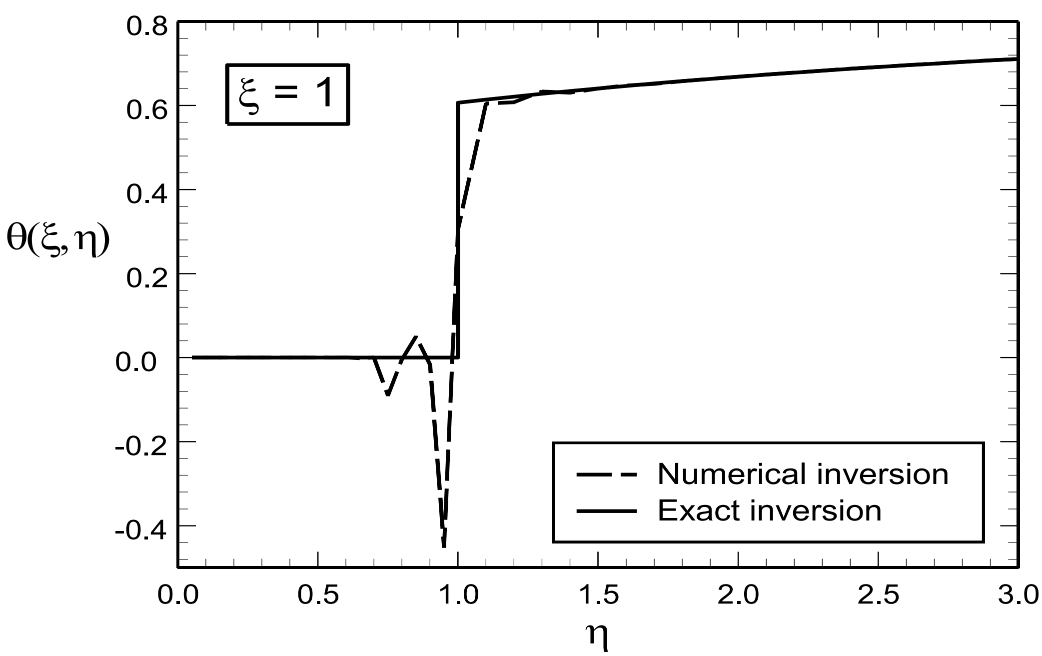

Figure 1.1 Dimensionless lattice temperatures as a function of η at selected ξ locations

CHAPTER 2

TEMPERATURE DISTRIBUTION IN SEMI-INFINITE BODIES IN THE PRESECENCE OF HEAT WAVES

2.1 Introduction

In this section, consideration is given to one-dimensional temperature solution in semi-infinite bodies. The temperature solutions for two cases are considered: (1) having a specified surface temperature and (2) having a prescribed surface heat flux. For both cases, it is hypothesized that the initial temperature is uniform with zero derivative with respect to time. As stated earlier, for thermal wave problems $\tau_t = 0$. Then, in a one-dimensional body, the governing equation becomes where *T* is the medium temperature that stands for the lattice temperature.

$$k\frac{\partial^2 T}{\partial x^2} + \left(S + \tau_q \frac{\partial S}{\partial t}\right) = C\left[\frac{\partial T}{\partial t} + \tau_q \frac{\partial^2 T}{\partial t^2}\right] \tag{2.1}$$

The work presented in this chapter is essentially done to emphasize on the thermal behavior of plate and a geometry consisting of two layers of dissimilar dielectric material. The cases discussed here have been previously investigated by other researchers in the past and their contribution is deeply appreciated. This chapter principally shows how Laplace transform method can be used to solve the problems accurately and efficiently.

2.2 Semi-Infinite body with specified surface temperature

The Figure 2.1 represents the geometry of the problem. It has an initial temperature T_i and a surface temperature jump T_o, when $t = 0$, it is convenient to define a dimensionless temperature $\theta = (T - T_i)/(T_O - T_i)$. Therefore, when the surface temperature has a constant value, the parameter T_O becomes the assigned surface temperature.

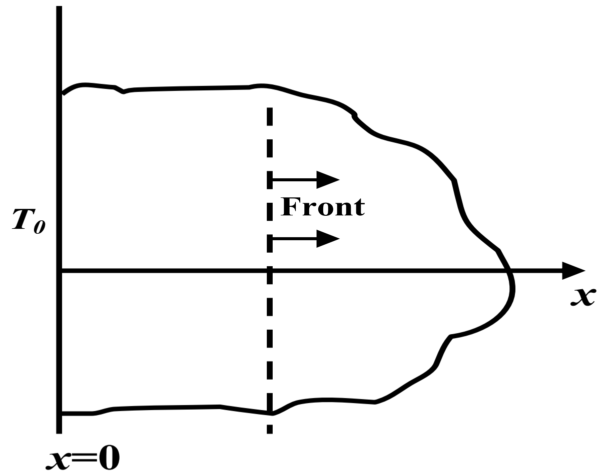

Figure 2.1 A semi-infinite body with temperature T_0 at the surface x=0.

Furthermore, in dimensionless space, one can set, $\xi = x/\sqrt{\alpha\tau_q}$ and, $\eta = t/\tau_q$ to get

$$\frac{\partial^2\theta}{\partial\xi^2} = \frac{\partial\theta}{\partial\eta} + \frac{\partial^2\theta}{\partial\eta^2} \quad \text{for } 0 \le \xi < \infty \tag{2.2}$$

Defining the Laplace Transform of $\theta(\xi,\eta)$ as $\bar{\theta}(\xi,s)$, then, the Laplace transform of Eq. (2.2), when $\theta(\xi,0) = 0$ and $\partial\theta/\partial\eta\,|_{\eta=0} = 0$ is

$$\frac{d^2\bar{\theta}}{d\xi^2} - \left(s + s^2\right)\bar{\theta} = 0 \quad \text{for} 0 \le \xi < \infty, \tag{2.3}$$

for a semi-infinite body. Equation (2.3) is an ordinary differential equation whose solution that satisfies the condition of finite $\theta(\xi,\eta)$, as $\xi \to \infty$, is

$$\bar{\theta} = A \exp\left[-\sqrt{s(s+1)}\ \xi\right] \tag{2.4}$$

The constant *A* in Eq. (2.4) depends on the surface condition, when $\xi = 0$. By placing a known dimensionless surface condition $\theta(0,\eta)$ in Eq. (2.4), it makes $A = \bar{\theta}(0,s)$ and then Eq. (2.4) takes the following form

$$\bar{\theta} = \bar{\theta}(0,s)\exp\left[-\sqrt{s(s+1)}\,\xi\right] \tag{2.5}$$

The inverse Laplace transforms of Eq. (2.5) is obtainable using a technique discussed in [17] as

$$L^{-1}\left\{\exp\left[-\sqrt{s(s+1)}\,\xi\right]\right\} = \exp\left[-\frac{\eta}{2}\right] \times \left\{\delta\left[\eta-\xi\right] + H(\xi-\eta)\frac{\xi}{2}\frac{I_1\left[\frac{1}{2}\sqrt{\eta^2-\xi^2}\right]}{\sqrt{\eta^2-\xi^2}}\right\} \tag{2.6}$$

where $\delta(\eta-\xi)$ is the Dirac delta function. This equation has a zero value when $\eta < \xi$. Then, the convolution theorem provides the temperature solution,

$$\theta(\xi,\eta) = \int_{\lambda=0}^{\eta} \theta(0,\eta-\lambda)\exp\left[-\frac{\lambda}{2}\right] \times \left\{\delta\left[(\lambda)-\xi\right] + H(\xi-\lambda)\frac{\xi}{2}\frac{I_1\left[\frac{1}{2}\sqrt{(\eta-\lambda)^2-\xi^2}\right]}{\sqrt{(\eta-\lambda)^2-\xi^2}}\right\} d\lambda \tag{2.7}$$

When the surface temperature T_0 is a constant, then using $T(0,\eta) = T_0$ to get $\theta(0,\eta) = 1$ and Eq. (2.7) becomes

$$\theta(x,t) = e^{-\xi/2} H(t/\tau_q - \xi) + \frac{1}{2}\xi \int_{\eta=\xi}^{t/\tau_q} \frac{e^{-\eta/2} I_1\left[\frac{1}{2}\sqrt{\eta^2-\xi^2}\right]}{\sqrt{\eta^2-\xi^2}} d\eta \tag{2.8}$$

where $H(t/\tau_q - \xi)$ is the Heaviside function. Figures 3.1 and 3.2 describes the numerical behaviors of Eq. (2.8) and it shows the variation of temperature as a function of time at different axial locations. This figure clearly demonstrates the existence of a temperature jump as the thermal wave arrives at any given location.

2.3 Semi-Infinite body with prescribed heat flux

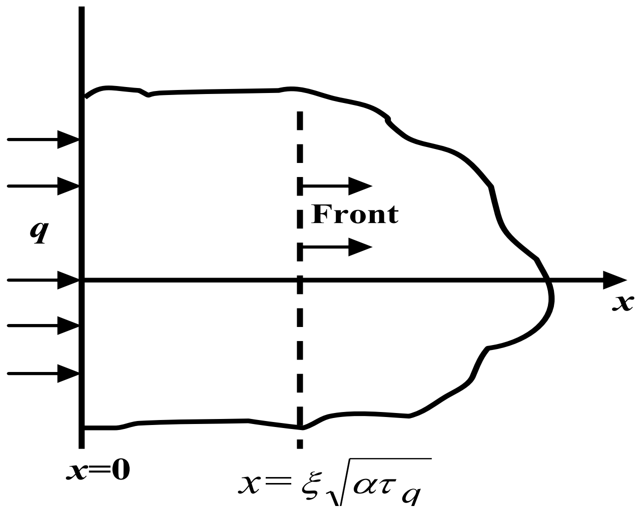

Figure 2.2 A semi-infinite body with heat flux *q* at the surface *x*=0

The thermal wave equation for the given example is given by:

$$k\frac{\partial^2 T}{\partial x^2}=C\frac{\partial T}{\partial t}+C\tau_q\frac{\partial^2 T}{\partial t^2} \tag{2.9}$$

Where *k* is thermal conductivity of the material, *C* is the capacitance and is equal to the product of the density (ρ) and specific heat of the material $(c_p)$and τ_q is the lag time due to heat flux. If one multiplies both sides of Eq. (2.9) by τ_q the hyperbolic form of the heat conduction equation takes the following form;

$$\alpha\tau_q\frac{\partial^2 T}{\partial x^2}=\tau_q\frac{\partial T}{\partial t}+\tau_q{}^2\frac{\partial^2 T}{\partial t^2} \tag{2.10}$$

Where $\alpha = k/C$, is the thermal diffusivity of the material. The Eq. (2.10) can be further reduced to a form where position (x) and time (t) are replaced by dimensionless variables in space (ξ) and time (η) defined as.

$$\xi \to \frac{x}{\sqrt{\alpha\tau_q}} \quad \text{and} \quad \eta \to \frac{t}{\tau_q} \tag{2.11}$$

The above transformations are made in Eq. (2.10) to become

$$\frac{\partial^2 T}{\partial \xi^2} = \frac{\partial T}{\partial \eta} + \frac{\partial^2 T}{\partial \eta^2} \tag{2.12}$$

A close examination of Eq. (2.12) can lead us to derive a dimensionless form of the thermal wave equation in a semi- infinite body. By replacing the temperature (T) with a dimensionless temperature variable (θ) where θ is given by,

$$\theta \to \frac{k(T - T_i)}{q\sqrt{\alpha\tau_q}} \tag{2.13}$$

where T_i is the initial temperature of the body and is assumed to be equal to zero.

$$\frac{\partial^2 \theta}{\partial \xi^2} = \frac{\partial \theta}{\partial \eta} + \frac{\partial^2 \theta}{\partial \eta^2} \tag{2.14}$$

The boundary conditions are given by a heat flux at x=0 is given by the following equation,

$$q + \tau_q \frac{\partial q}{\partial t} = -k\frac{\partial T}{\partial x} \tag{2.15.1}$$

A careful observation would lead us to a conclusion that there exists a lag time due to the heat flux. This means that after a pulse has been generated at the surface at x=0 it takes sometime before there is considerable jump in temperature on that surface. Thus we hypothesize the heat flux q to be a pulse and mathematically we define it by a step function defined as follows:

$$q = S_0(t) = \begin{cases} 0 & t < 0 \\ q & t \ge 0 \end{cases} \tag{2.15.2}$$

Now, after replacing the variables in Eq. (2.15.1) with the dimensionless variable in space (ξ), time (η) and temperature (θ) it takes the following form,

$$-\frac{\partial\theta}{\partial\xi} = 1 + \delta(\eta - 0) \tag{2.16}$$

Note I: L $\{\delta(t-\tau)\} = e^{-s\tau}, t \geq 0$

In the given example $\tau = 0$ *and thus the Laplace transform of the Dirac delta function gives us unity, L* $\{\delta(t-0)\} = 1.$

Observe that the first term of Eqn. (2.15.1) becomes a Dirac delta function because thee differentiation of a Step function results into a Dirac delta function [18]. Let $\bar{\theta}$ denote the Laplace transform of θ, ($\bar{\theta}$ =*L* {θ}). Now taking a Laplace transform of Eq. (2.15.2), we obtain,

$$-\frac{\partial\bar{\theta}}{\partial\xi} = \frac{1}{s} + 1 \tag{2.17}$$

Thus we proceed by taking Laplace transform of the Eq. (2.15.1),

$$\frac{\partial^2\bar{\theta}}{\partial\xi^2} = s\bar{\theta} + s^2\bar{\theta} \tag{2.18}$$

Solving the differential equation Eq. (2.14) we obtain the following solution,

$$\bar{\theta} = C_1\, Exp\,[\sqrt{s+s^2}\,\xi] + C_2\, Exp\,[-\sqrt{s+s^2}\,\xi] \tag{2.19}$$

Now by setting ξ to positive infinity one can predict that the value of the constant C_1 goes to zero. Thus the solution reduces to,

$$\bar{\theta} = C_2\ Exp\ [-\sqrt{s+s^2}\,\xi] \tag{2.20}$$

The value of the constant C_2 can be determined by applying the boundary condition at *x*=0; that is, ξ=0. By placing $\bar{\theta}$ from Eq. (2.20) into Eq. (2.16) one can compute the value of the constant C_2.

$$-\left.\frac{\partial\left(C_2 Exp[-\sqrt{s+s^2}\,\xi]\right)}{\partial\xi}\right|_{\xi=0} = \frac{1}{s}+1 \tag{2.21}$$

From Eq. (2.21) we have,

$$C_2\sqrt{s+s^2} = \frac{1}{s}+1 \tag{2.22}$$

$$C_2 = \frac{1}{s\sqrt{s+s^2}}+\frac{1}{\sqrt{s+s^2}} \tag{2.23}$$

Substituting the value of C_2 obtained from Eq. (2.23) in Eq. (2.20) to obtain an expression for $\bar{\theta}$,

$$\bar{\theta} = \left[\frac{1}{s\sqrt{s+s^2}}+\frac{1}{\sqrt{s+s^2}}\right] Exp\ [-\sqrt{s+s^2}\,\xi] \tag{2.24}$$

By taking Laplace inversion of Eq. (2.24) we obtain the dimensionless temperature profile in a semi-infinite body. Further reducing Eq. (2.24) would result in a form whose Laplace inversion can be easily obtained from standard Laplace Transform Tables, e.g., from Eq. (88) in Appendix 3 of [18] as

$$\bar{\theta} = \frac{1}{s\sqrt{s+s^2}} Exp\ [-\sqrt{s+s^2}\,\xi] + \frac{1}{\sqrt{s+s^2}} Exp\ [-\sqrt{s+s^2}\,\xi] \tag{2.25}$$

Note II: The terms within this equation have the forms whose inverse Laplace transforms are obtainable using relation,

$$L^{-1}\left\{\frac{\exp[-\kappa\sqrt{s(s+a)}]}{\sqrt{s(s+a)}}\right\} = \begin{cases} 0 & \text{when } 0 < t < \kappa \\ e^{-at/2} I_0\left(\frac{a}{2}\sqrt{t^2-\kappa^2}\right) & \text{when } t > \kappa \end{cases} \tag{2.26}$$

Following the procedure stated in *Note II* and applying the same to Eq. (2.25) we deduce the temperature profile.

$$\theta = \int_{t_d}^{t_f} e^{-\frac{\eta}{2}} I_0\left[\frac{1}{2}\sqrt{\eta^2-\xi^2}\right] d\eta + e^{-\frac{\eta}{2}} I_0\left[\frac{1}{2}\sqrt{\eta^2-\xi^2}\right] \tag{2.27}$$

The first term of the Eq. (2.27) is an integral because of applying convolution integral theorem to the first term of Eq. (2.26).

2.4 Conclusion

In this chapter analytical solutions were obtained for a semi-infinite dielectric body with boundary conditions of first and second kind. They are given by Eq. (2.7) and Eq. (2.27) in the chapter. It has been well illustrated in this chapter how the classical method of Laplace transform was used to derive the temperature solution. The formulated equations are now going to be used to predict the temperature field in the dielectric substance. The analysis of these equations will be done in the following chapter with the help of several illustrations and data of several cases which has been presented in tabular form as well. The work in this chapter is to examine the thermal behavior of the given geometry and also to emphasize on the thermal behavior of a dielectric plate. These observations will be discussed later in the study.

CHAPTER 3

ANALYSIS OF TEMPERATURE DISTRIBUTION DUE TO THE OCCURENCE OF A THERMAL WAVE IN SEMI-INFINITE BODIES

3.1 Introduction

In this chapter we are going to examine the thermal behavior of a semi-infinite dielectric material when it is subjected to different boundary conditions as discussed in the previous chapter. The work presented in this chapter has been studied earlier by different researchers but it has been worked on again in order to emphasize on the thermal behavior for dielectric material of finite size. As the mathematical formulation was presented and analytical solutions were obtained prior to this section, we have used them to develop several Mathematica subroutines that are presented in Appendix A of the work.

The first sub-section shows the variation in temperature distribution in dimensionless space (ξ) holding the dimensionless time (η) constant. Thus for different values of η several temperature profiles for the case temperature prescribed on the surface of a dielectric semi-infinite body were plotted as shown in Figure 3.1. The results obtained have a good agreement with those available in the literature.

The subsequent part essentially focuses on the case when heat flux has been specified on the surface of the dielectric material. For a specified time it has been shown how the jump in temperature takes place inside the material. The jump in temperature has been well illustrated later in the chapter with the help of figures. Also the hyperbolic nature of the thermal wave equation is shown in Figure 3.2 when the wave is travelling inside the substance. The results are presented in tabulated form and by witnessing the nature of the plots and on comparing them with other previous studies a resilient similarity between the results was perceived.

3.2 Analysis of thermal behavior for X10 case

In this section analysis has been done for specified wall temperature at the surface of a dielectric substance as discussed earlier in section 2.1 of Chapter 2. The results that are presented in Table 3.1 were obtained from the developed Mathematica subroutine presented in Appendix A of the study. In an attempt to acquire better accuracy huge quantity of data were generated for different specified dimensionless time but a few of those obtained results have been represented in Table 3.1.

Table 3.1 Dimensionless temperature distribution in a semi-infinite body with boundary condition of first kind for different dimensionless time in a dimensionless space.

η = 1		η = 2		η = 3		η = 4	
ξ	θ	ξ	θ	ξ	θ	ξ	θ
0	0	0	0	0	0	0	0
0.0125	0.00054796	0.0375	0.0010759	0.0625	0.0012422	0.0875	0.00126677
0.025	0.0010959	0.075	0.0021515	0.125	0.0024836	0.175	0.00253193
0.0375	0.00164381	0.1125	0.0032266	0.1875	0.0037232	0.2625	0.0037939
0.05	0.00219167	0.15	0.0043008	0.25	0.0049603	0.35	0.00505108
0.0625	0.00273947	0.1875	0.0053739	0.3125	0.0061941	0.4375	0.00630188
0.075	0.00328719	0.225	0.0064457	0.375	0.0074236	0.525	0.00754474
0.0875	0.00383481	0.2625	0.0075158	0.4375	0.0086481	0.6125	0.00877807
0.1	0.00438232	0.3	0.008584	0.5	0.0098667	0.7	0.0100003
0.125	0.00547695	0.3375	0.00965	0.5625	0.0110786	0.7875	0.01121
0.15	0.00657093	0.375	0.0107135	0.625	0.012283	0.875	0.0124056
0.175	0.00766415	0.45	0.0128321	0.75	0.0146658	1.05	0.0147484

Table 3.1 – continued

$\eta = 1$		$\eta = 2$		$\eta = 3$		$\eta = 4$	
ξ	θ	ξ	θ	ξ	θ	ξ	θ
0.2	0.00875648	0.525	0.0149376	0.875	0.0170088	1.225	0.0170172
0.225	0.00984779	0.5625	0.0159847	0.9375	0.0181634	1.3125	0.0181202
0.25	0.0109379	0.6	0.0170278	1	0.0193057	1.4	0.0192006
0.275	0.0120268	0.6375	0.0180665	1.0625	0.0204349	1.4875	0.020257
0.3	0.0131143	0.675	0.0191006	1.125	0.0215502	1.575	0.0212881
0.35	0.0152846	0.7125	0.0201299	1.1875	0.022651	1.6625	0.0222926
0.375	0.0163671	0.75	0.0211539	1.25	0.0237364	1.75	0.0232694
0.4	0.0174477	0.7875	0.0221726	1.3125	0.0248058	1.8375	0.0242173
0.425	0.0185263	0.825	0.0231857	1.375	0.0258584	1.925	0.0251351
0.45	0.0196027	0.8625	0.0241928	1.4375	0.0268936	2.0125	0.0260218
0.475	0.0206769	0.9	0.0251938	1.5	0.0279106	2.1	0.0268763
0.5	0.0217486	0.9375	0.0261883	1.5625	0.0289088	2.1875	0.0276977
0.5	0.800549	0.975	0.0271762	1.625	0.0298875	2.275	0.0284849
0.525	0.790675	1.0125	0.0281572	1.75	0.0317841	2.3625	0.0292372
0.55	0.780815	1.05	0.0291309	1.875	0.0335953	2.45	0.0299536
0.575	0.77097	1.0875	0.0300973	2	0.0353165	2.5375	0.0306335
0.6	0.76114	1.125	0.031056	2.0625	0.0361419	2.625	0.0312759
0.625	0.751327	1.1625	0.0320068	2.125	0.0369433	2.7125	0.0318804
0.65	0.741531	1.2	0.0329495	2.1875	0.03772	2.8	0.0324462
0.675	0.731752	1.275	0.0348095	2.25	0.0384717	2.8875	0.0329728
0.7	0.721991	1.3125	0.0357263	2.3125	0.0391977	2.975	0.0334597
0.725	0.71225	1.35	0.0366341	2.375	0.0398978	3.0625	0.0339065

Table 3.1 – continued

***η* = 1**		***η* = 2**		***η* = 3**		***η* = 4**	
ξ	***θ***	***ξ***	***θ***	***ξ***	***θ***	***ξ***	***θ***
0.75	0.702528	1.425	0.0384215	2.4375	0.0405714	3.15	0.0343127
0.775	0.692827	1.4625	0.0393007	2.5	0.0412181	3.2375	0.0346779
0.8	0.683146	1.5	0.0401699	2.5	0.327723	3.325	0.035002
0.825	0.673487	1.5	0.512536	2.5625	0.313909	3.4125	0.0352848
0.85	0.66385	1.575	0.490038	2.625	0.3003	3.5	0.035526
0.875	0.654236	1.65	0.467805	2.6875	0.2869	3.5	0.2093
0.9	0.644645	1.725	0.445849	2.75	0.273712	3.5875	0.195454
0.925	0.635079	1.8	0.424181	2.8125	0.260738	3.675	0.181988
0.95	0.625537	1.875	0.40281	2.875	0.247981	3.7625	0.168905
0.975	0.616021	1.95	0.381746	2.9375	0.235445	3.85	0.156206
1	0.606531	2	0.367879	3	0.22313	4	0.135335
1	0	2	0	3	0	4	0

The data presented in the above table corresponds to Figure 3.2 of the study. As mentioned earlier a sample of data has been presented in order to locate the position inside the body where the jump in temperature occurs at a fixed time which was specified by us for each simulation. The data obtained for each dimensionless time was thoroughly examined. The Figure 3.1 has also been plotted with the aid of the same data by not introducing a time delay. Figure 3.1 and Figure 3.2 are discussed in detail below.

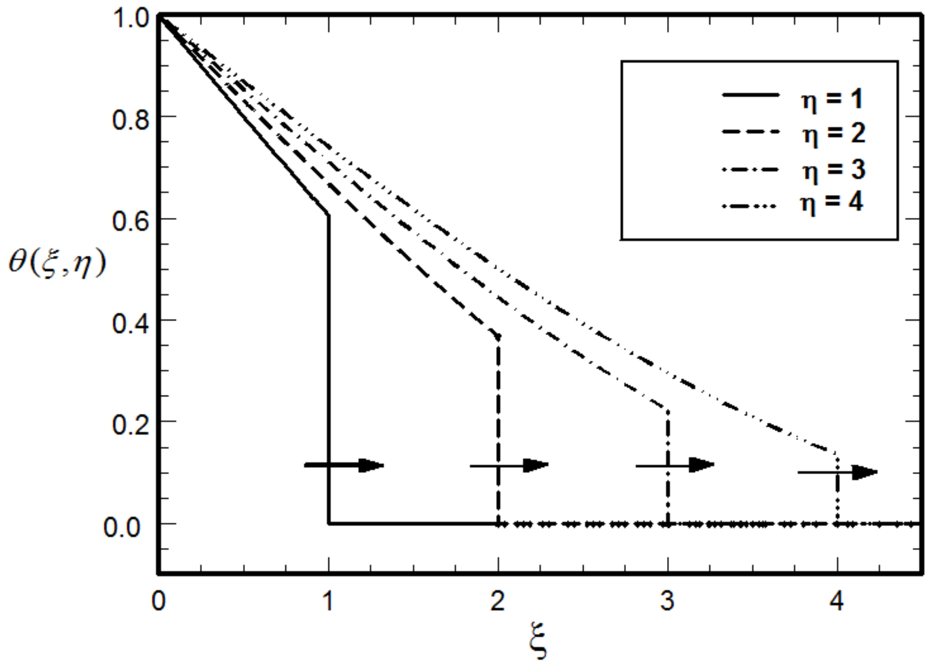

Figure 3.1 Front travelling with finite speed in a semi-infinite body with specified temperature at the wall for different dimensionless time in dimensionless space.

The Figure 3.1 noticeably shows the front moving forward due to sudden change in wall temperature. Here we have graphically represented the temperature profile for four different time in space when $x > 0$. We observe that for each case the dimensionless temperature rises up rapidly to 1 at $x = 0$ followed by heat conduction which is hyperbolic in nature. Also there is a sudden drop in temperature when the value of ξ becomes equal to the specified value of η. In the figure the wave travels in the direction of the arrowhead. Since we hold the temperature constant at the wall and the geometry being semi-infinite we see that the effect of hyperbolic heat conduction reduces and diffusion slowly takes over as time increases and finally the temperature of the body becomes equal to the wall temperature for very large times.

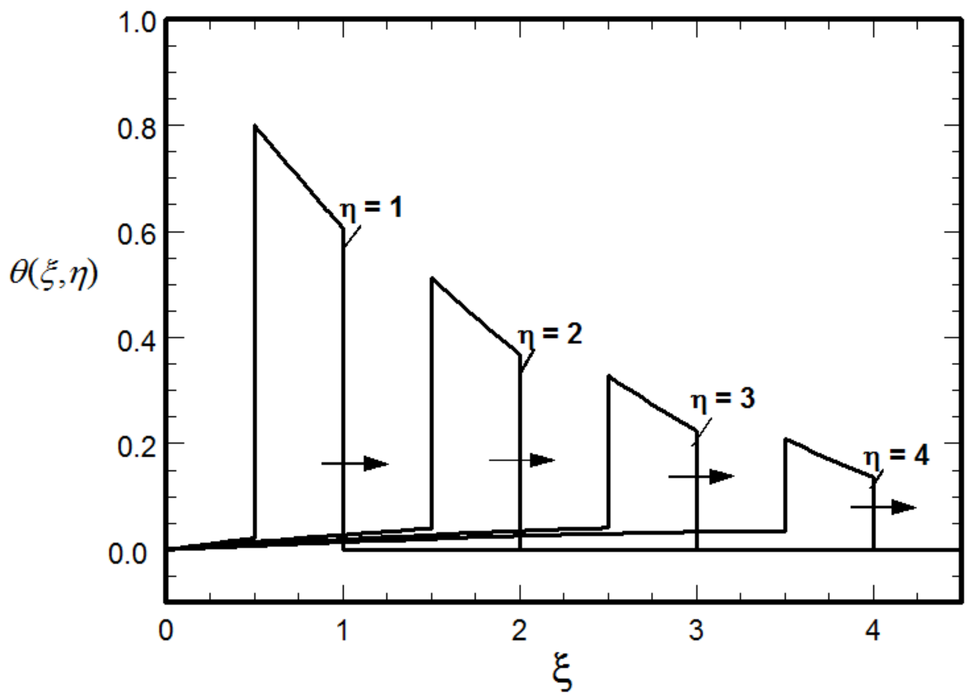

Figure 3.2 Dimensionless temperature profiles with uniform pulse width in a semi-infinite body under the effect of constant wall temperature.

Figure 3.2 is an alternate way of graphically representing the effect of hyperbolic heat conduction. The difference between Figure 3.2 and 3.1 is essentially we try to plot the graph between two time intervals. For instance, referring Figure 3.2, we notice that the temperature monotonically increases till ξ = 0.5 where the jump in temperature takes place. The jump takes place because we specify η to be as 0.5. From Table 3.1 we see that at ξ = 0.5 the value of θ changes from 0.0217486 to 0.800549. We observe gradual decrease in temperature till η =1 when the temperature drops down to zero. This explanation holds good for all the other values of η that are represented in the figure.

In dielectric materials the energy carriers are essentially phonons and it would be agreeable to comment on the energy between two consequent values of η. Notice that the pulse width is uniform for each one but the height of the pulse changes. As η increases the height of the pulse decreases but notice that distance travelled by the wave for the pulse to occur for a larger value of η is more that compared to a much lower value. This has been well illustrated in Figure 3.2. Hence the area under the curve remains the same for each time of travel. In other words the difference in the height of two neighboring pulses is adjusted with the length of the wave travel before the jump in temperature occurs for a specified value of η .

3.3 Analysis of thermal behavior for X20 case

In this section analysis has been done when heat flux strikes the surface of a dielectric substance at x = 0 and t = 0as discussed earlier in section 2.2, Chapter 2. The results that are presented in Table 3.2 were obtained from the developed Mathematica subroutine presented in Appendix A of the study. In an attempt to acquire better accuracy huge quantity of data were generated for different specified dimensionless time but a few of those obtained results have been represented in Table 3.2 and Table 3.3. The Figure 3.2 and Figure 3.3 were plotted using the entire data set that was obtained after the simulation.

Table 3.2 Dimensionless temperature distribution in a semi-infinite body with boundary condition of second kind for different dimensionless time in a dimensionless space.

η = 1		**η = 2**		**η = 3**		**η = 4**	
ξ	**θ**	**ξ**	**θ**	**ξ**	**θ**	**ξ**	**θ**
0	1.44649	0	1.8131	0	2.12685	0	2.40362
0.025	1.42159	0.075	1.7389	0.0625	2.06485	0.0875	2.31702
0.05	1.39689	0.15	1.6663	0.125	2.00386	0.175	2.23222
0.075	1.3724	0.225	1.59531	0.1875	1.94386	0.2625	2.14921
0.1	1.3481	0.3	1.52591	0.25	1.88487	0.35	2.068
0.125	1.32401	0.375	1.45811	0.3125	1.82688	0.4375	1.98858
0.15	1.30012	0.45	1.3919	0.375	1.76989	0.525	1.91095

Table 3.2 – continued

***η* = 1**		***η* = 2**		***η* = 3**		***η* = 4**	
ξ	***θ***	***ξ***	***θ***	***ξ***	***θ***	***ξ***	***θ***
0.175	1.27643	0.525	1.32728	0.4375	1.71389	0.6125	1.83511
0.2	1.25294	0.6	1.26425	0.5	1.6589	0.7	1.76104
0.225	1.22965	0.675	1.2028	0.5625	1.60489	0.875	1.61821
0.25	1.20657	0.75	1.14292	0.625	1.55188	0.9625	1.54943
0.275	1.18368	0.825	1.0846	0.6875	1.49986	1.05	1.4824
0.3	1.16099	0.9	1.02784	0.75	1.44882	1.225	1.35354
0.325	1.13851	0.9375	1.00005	0.8125	1.39876	1.4	1.23153
0.35	1.11623	0.975	0.972639	0.875	1.34969	1.575	1.11629
0.375	1.09414	1.05	0.918976	0.9375	1.30159	1.6625	1.06116
0.4	1.07226	1.125	0.866845	1	1.25446	1.75	1.00768
0.425	1.05058	1.2	0.816236	1.125	1.1631	1.8375	0.955837
0.45	1.0291	1.275	0.767138	1.25	1.07558	1.925	0.905602
0.475	1.00781	1.35	0.719541	1.375	0.991849	2.0125	0.856964
0.5	0.98673	1.425	0.673431	1.4375	0.951391	2.1	0.809904
0.525	0.965845	1.5	0.628796	1.5	0.911865	2.275	0.720443
0.55	0.94516	1.575	0.585623	1.625	0.83558	2.45	0.637062
0.575	0.924674	1.65	0.543898	1.75	0.762941	2.625	0.559596
0.6	0.904386	1.725	0.503606	1.8125	0.727972	2.7125	0.523027
0.65	0.864405	1.8	0.464732	1.875	0.693893	2.8	0.48787
0.7	0.825215	1.875	0.42726	1.9375	0.660697	2.975	0.421701
0.75	0.786813	1.95	0.391175	2	0.628375	3.0625	0.390641
0.8	0.749196	2	0.367879	2.25	0.507676	3.15	0.360898

Table 3.2 – continued

$\eta = 1$		$\eta = 2$		$\eta = 3$		$\eta = 4$	
ξ	θ	ξ	θ	ξ	θ	ξ	θ
0.85	0.712363	2	0	2.5	0.400302	3.325	0.305265
0.9	0.67631	1.875	0.40281	2.625	0.351429	3.5	0.254599
0.95	0.641034	1.95	0.381746	2.75	0.305664	3.85	0.167331
1	0.606531	2	0.367879	3	0.22313	4	0.135335
1	0	2	0	3	0	4	0

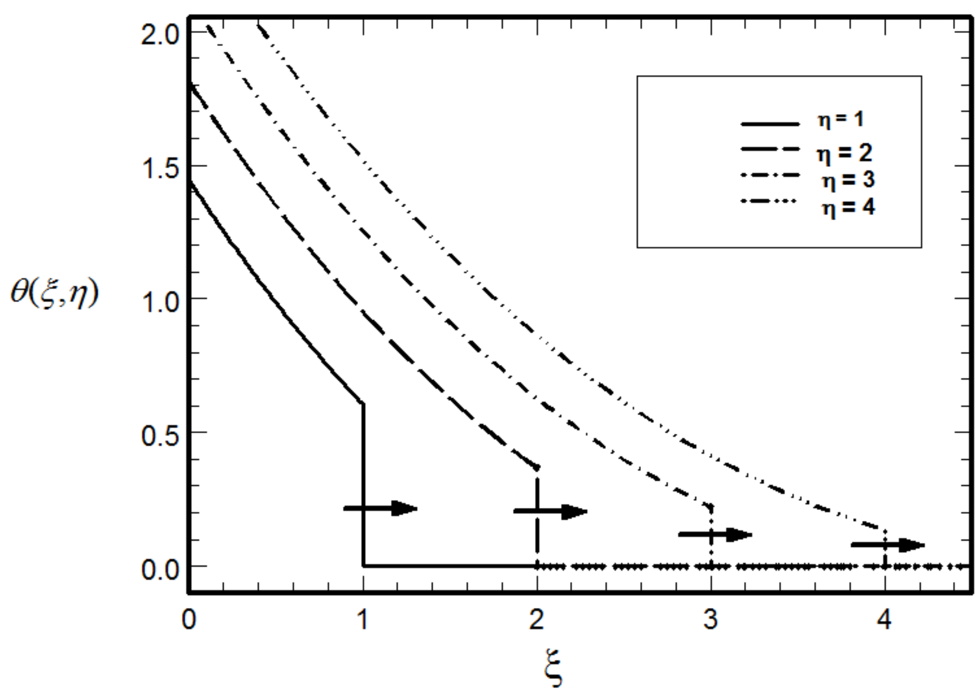

Figure 3.3 Front moving with finite speed in a semi-infinite body under the influence of a prescribed heat flux for different dimensionless time in dimensionless space.

The figure above represents the behavior of a semi-infinite dielectric material when subjected to a heat flux. The Figure 3.3 corresponds to Table 3.2. The graph is similar to Figure 3.1 apart from a noticeable change, that is the surface temperature of the body at x = 0. The reason for the increase in surface temperature is because initially after heat flux comes in through the surface at x = 0, we cut it off. The heat that is stored in the body after each pulse has been generated is the cause for the rise in surface temperature. The area under each curve represents the energy stored inside the body after each pulse has been generated. As commented earlier for Figure 3.1 that diffusion process takes over as time increases the same can be understood for this case.

Table 3.3 Dimensionless temperature distribution with uniform pulse width $\Delta\xi$ in a semi-infinite body with prescribed heat flux.

***η* = 1**		***η* = 2**		***η* = 3**		***η* = 4**	
ξ	***θ***	***ξ***	***θ***	***ξ***	***θ***	***ξ***	***θ***
0	0.210909	0	0.175355	0	0.151447	0	0.134476
0.05	0.210879	0.075	0.175306	0.125	0.151344	0.175	0.134319
0.1	0.21079	0.15	0.17516	0.25	0.151037	0.35	0.133851
0.15	0.21064	0.225	0.174915	0.375	0.150527	0.525	0.133072
0.2	0.2104314	0.3	0.174574	0.5	0.149814	0.7	0.131987
0.25	0.210162	0.375	0.174136	0.625	0.1489	0.875	0.130601
0.275	0.210005	0.45	0.173601	0.75	0.147788	1.05	0.128919
0.3	0.209834	0.525	0.17297	0.875	0.146481	1.225	0.126951
0.35	0.209446	0.6	0.172244	1	0.144981	1.3125	0.125861
0.4	0.209	0.675	0.171423	1.125	0.143293	1.4	0.124704
0.45	0.208493	0.75	0.170508	1.25	0.141421	1.575	0.122189
0.5	0.207929	0.825	0.1695	1.375	0.139369	1.75	0.119417

Table 3.3 – continued

$\eta = 1$		$\eta = 2$		$\eta = 3$		$\eta = 4$	
ξ	θ	ξ	θ	ξ	θ	ξ	θ
0.525	0.965845	0.9	0.1684	1.5	0.137142	1.925	0.116402
0.55	0.94516	0.975	0.167209	1.625	0.134747	2.0125	0.114807
0.575	0.924674	1.05	0.165928	1.75	0.132189	2.275	0.109695
0.6	0.904386	1.125	0.164558	1.875	0.129474	2.45	0.106034
0.70	0.825215	1.425	0.158221	2.375	0.117188	2.975	0.0940161
0.8	0.749196	1.5	0.628796	2.5	0.400302	3.325	0.0853212
0.9	0.67631	1.8	0.464732	2.75	0.305664	3.675	0.208691
1	0.606531	2	0.367879	3	0.22313	4	0.135335
1	0	2	0	3	0	4	0

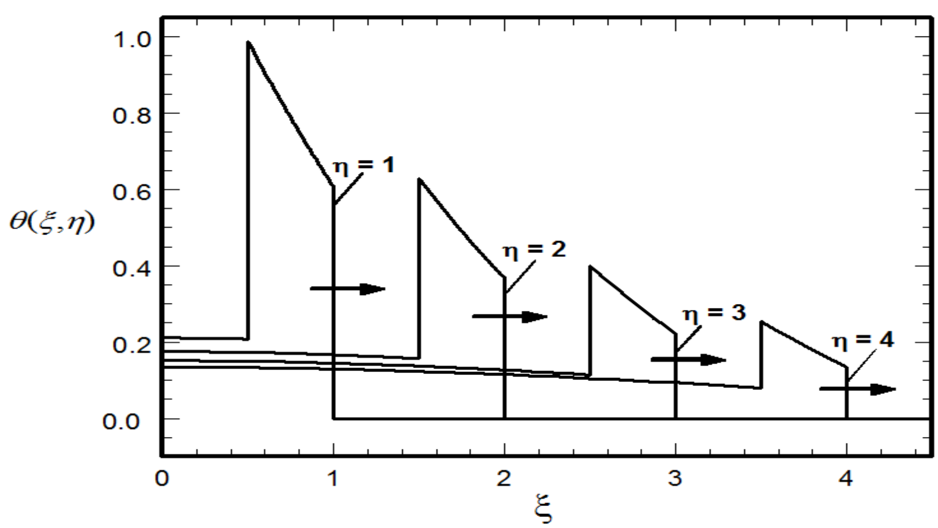

Figure 3.4 Dimensionless temperature profiles with uniform pulse width $\Delta\xi$ in a semi-infinite body under the effect of a prescribed heat flux.

Figure 3.4 is an alternate way of graphically representing the effect of hyperbolic heat conduction. The difference between Figure 3.4 and 3.3 is that in the later, we essentially try to plot the graph between two time intervals. For instance referring to Figure 3.4, we notice that the temperature monotonically decreases till ξ = 0.5 where the jump in temperature takes place because η was specified to be 0.5. From Table 3.3 we see that at ξ = 0.5 the value of θ changes from 0.207929 to 0.965845. We observe significant drop in temperature till η =1 after which the temperature drops down to zero. This explanation holds good for all the other values of η that are represented in the figure.

In this case the pulse width of $\Delta\xi$ is kept uniform but the height of the pulse shrinks like before as η increases. The energy that is generated after each pulse can be calculated by considering a differential element of width $d\xi$ inside the pulse and integrating it over the entire pulse width. This should be equal to the heat flux coming in at that particular time and thus first law of thermodynamics holds good. As mentioned in the previous case the effect of hyperbolic heat conduction decreases as time increases.

3.4 Conclusion

Analytical solutions that were obtained in Chapter 2 were analyzed successfully and the results were compared with previous works that were available in the literature. The acquired results were in good agreement with the existing solution and hence the objective was achieved. As we said earlier that the analysis of this section was done in order to verify the results for a finite body under special circumstances. Also the physics behind the occurrence of the phenomena of Hyperbolic Heat Conduction was examined in detail and grasped.

.

CHAPTER 4

TEMPERATURE SOLUUTION IN FINITE BODIES IN THE

PRESECENCE OF A HEAT WAVE

4.1 Introduction

In this Chapter we are going to discuss about a flat thin plate made of a dielectric substance when subjected to rapid heating. Boundary conditions of first and second kind are considered to solve the particular boundary value problem. The use of dimensionless parameters is encouraged because we are heating a sub-micron substance in very small time.

4.2 Thermal Wave in a plate with prescribed heat flux on the surface

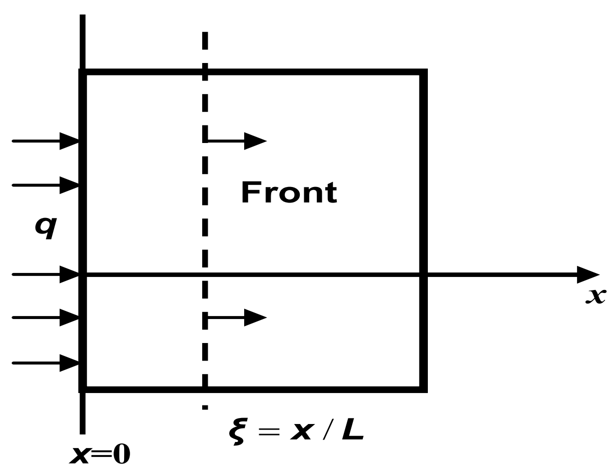

Figure 4.1 Geometry of a flat dielectric plate with heat flux *q* at the surface *x*=0.

The thermal wave equation in a finite body (plate) is given by the same equation that for a semi-infinite body; that is, Eq. (2.1). Since there is no volumetric heat source present in the problem we can neglect that take the effect of source into consideration.

Thus we finally obtain,

$$k\frac{\partial^2 T}{\partial x^2} = C\frac{\partial T}{\partial t} + C\tau_q \frac{\partial^2 T}{\partial t^2}$$

$$\frac{\partial^2 T}{\partial x^2} = \frac{1}{\alpha}\frac{\partial T}{\partial t} + \frac{\tau_q}{\alpha}\frac{\partial^2 T}{\partial t^2} \tag{4.1}$$

Multiplying both sides of Eq. (4.1) by L^2 we obtain,

$$L^2\frac{\partial^2 T}{\partial x^2} = \frac{L^2}{\alpha}\frac{\partial T}{\partial t} + \frac{\tau_q L^2}{\alpha}\frac{\partial^2 T}{\partial t^2} \tag{4.2}$$

$$\frac{\partial^2 T}{\partial\left(\frac{x^2}{L^2}\right)} = \frac{\partial T}{\partial\left(\frac{\alpha t}{L^2}\right)} + \frac{\alpha\tau_q}{L^2}\frac{\partial^2 T}{\partial\left(\frac{\alpha t}{L^2}\right)^2} \tag{4.3}$$

Following the same procedure that was adopted to solve for the temperature in a semi-infinite body we need to first convert Eq. (4.3) into a dimensionless form. This can be achieved by making the following transformations,

$$\xi \to \frac{x}{L} \qquad \eta \to \frac{\alpha t}{L^2} \qquad \tau_q{}^* \to \frac{\alpha\tau_q}{L^2} \tag{4.4}$$

where ξ is a dimensionless variable in space (*x*), η is a dimensionless variable in time (*t*) and $\tau_q{}^*$ is the dimensionless lag time due to heat flux.

$$\frac{\partial^2 T}{\partial \xi^2} = \frac{\partial T}{\partial \eta} + \tau_q{}^*\frac{\partial^2 T}{\partial \eta^2} \tag{4.5}$$

Further one can reduce Eq. (4.5) by multiplying with a factor $\frac{k}{qL}$ and θ, the dimensionless variable for temperature is given by the form,

$$\theta \rightarrow \frac{k(T - T_i)}{qL} \tag{4.6}$$

where *k* is the thermal conductivity if the slab, *T* is the temperature of the slab, T_i is the initial temperature of the slab, *q* is the heat flux and *L* is the length of the slab. Hence the final form of the thermal wave equation in dimensionless form becomes,

$$\frac{\partial^2 \theta}{\partial \xi^2} = \frac{\partial \theta}{\partial \eta} + \tau_q^* \frac{\partial^2 \theta}{\partial \eta^2} \tag{4.7}$$

The following step is to alter the boundary conditions from the regular form to a dimensionless form. To solve the above differential equation, Eq. (4.7) we need two boundary conditions, one at *x*=0 and another one at *x*=*L*. The boundary conditions specified at *x*=0 is that of a heat flux (*q*) entering the surface at time *t*=0. The mathematical representation of the above statement would be,

$$q + \tau_q \frac{\partial q}{\partial t} = -k \frac{\partial T}{\partial x} \tag{4.8}$$

Working on Eq. (4.8) one can make some modifications to achieve a dimensionless form.

$$q + \left(\frac{\alpha \tau_q}{L^2}\right)\left(\frac{L^2}{\alpha}\right)\frac{\partial q}{\partial t} = -\left(\frac{k}{L}\right)\frac{\partial T}{\partial \left(\frac{x}{L}\right)} \tag{4.9}$$

$$q + \left(\frac{\alpha \tau_q}{L^2}\right)\frac{\partial q}{\partial \left(\frac{\alpha t}{L^2}\right)} = -\left(\frac{k}{L}\right)\frac{\partial T}{\partial \left(\frac{x}{L}\right)} \tag{4.10}$$

Now closely observing Eq. (4.10) we see that there are a few terms that can be replaced by using Eq. (4.4). After doing so Eq. (4.10) appears with the dimensionless parameters ξ, η and τ_q^*.

$$q + \tau_q^* \frac{\partial q}{\partial \eta} = -\left(\frac{k}{L}\right)\frac{\partial T}{\partial \xi} \tag{4.11}$$

A careful examination of Eq. (4.11) would lead us back to Eq. (2.15.2) and we deduce the following,

$$q\left\{1+\tau_q{}^{*}\delta(\eta-0)\right\}=-\left(\frac{k}{L}\right)\frac{\partial T}{\partial \xi} \tag{4.12}$$

$$1+\tau_q{}^{*}\delta(\eta-0)=-\frac{\partial(kT/qL)}{\partial \xi} \tag{4.13}$$

The term on the right hand side of Eq. (4.13) can be replaced by the dimensionless temperature variable θ, refer Eq. (4.6). Hence the final form of Eq. (4.8) in dimensionless form is represented as,

$$1+\tau_q{}^{*}\delta(\eta-0)=-\frac{\partial \theta}{\partial \xi} \tag{4.14}$$

Thus one can write the boundary condition at *x*=0; that is, ξ =0 as,

$$-\left.\frac{\partial \theta}{\partial \xi}\right|_{\xi=0}=1+\tau_q{}^{*}\delta(\eta-0) \tag{4.15}$$

Now the surface at *x*=*L*; that is, ξ =1 is considered to be as insulated. The mathematical representation of the earlier statement is,

$$\left.\frac{\partial T}{\partial x}\right|_{x=L}=0 \qquad \text{Hence,} \quad \left.\frac{\partial \theta}{\partial \xi}\right|_{\xi=1}=0 \tag{4.16}$$

Subsequently we take the Laplace transform of the equations, Eq. (4.7), Eq. (4.15) and Eq. (4.16) and obtain a new set of equations.

$$\frac{\partial^2 \overline{\theta}}{\partial \xi^2}=s\,\overline{\theta}+s^2\tau_q{}^{*}\,\overline{\theta} \tag{4.17}$$

$$\frac{\partial^2 \overline{\theta}}{\partial \xi^2}=\left(s+s^2\tau_q{}^{*}\right)\overline{\theta} \tag{4.18}$$

$$-\left.\frac{\partial \overline{\theta}}{\partial \xi}\right|_{\xi=0}=\frac{1}{s}+\tau_q{}^{*} \tag{4.19}$$

$$\left.\frac{\partial\bar{\theta}}{\partial\xi}\right|_{\xi=1}=0 \tag{4.20}$$

Solution to the Eq. (4.18) is given by,

$$\bar{\theta}=A\cosh\left[\sqrt{s+s^2\tau_q{}^*}\,\xi\right]+B\sinh\left[\sqrt{s+s^2\tau_q{}^*}\,\xi\right] \tag{4.21}$$

Applying the boundary condition 1; that is, Eq. (4.19) to Eq. (4.21) one can derive the value for the coefficient *B*.

$$-B\sqrt{s+s^2\tau_q{}^*}=\frac{1}{s}+\tau_q{}^* \tag{4.22}$$

$$B=-\frac{1}{\sqrt{s+s^2\tau_q{}^*}}\left[\frac{1}{s}+\tau_q{}^*\right] \tag{4.23}$$

Replacing *B* obtained in Eq. (4.23) in Eq. (4.21), the equation becomes,

$$\bar{\theta}=A\cosh\left[\sqrt{s+s^2\tau_q{}^*}\,\xi\right]-\frac{1}{\sqrt{s+s^2\tau_q{}^*}}\left[\frac{1}{s}+\tau_q{}^*\right]\sinh\left[\sqrt{s+s^2\tau_q{}^*}\,\xi\right] \tag{4.24}$$

Applying the second boundary condition at x=L; that is, ξ =1 given by Eq. (4.20) to Eq. (4.24) one can obtain the value for the constant *A*.

$$A.\sinh\left[\sqrt{s+s^2\tau_q{}^*}\right]-\frac{1}{\sqrt{s+s^2\tau_q{}^*}}\left[\frac{1}{s}+\tau_q{}^*\right].\cosh\left[\sqrt{s+s^2\tau_q{}^*}\right]=0 \tag{4.25}$$

$$A=\frac{1}{\sqrt{s+s^2\tau_q{}^*}}\left[\frac{1}{s}+\tau_q{}^*\right].\coth\left[\sqrt{s+s^2\tau_q{}^*}\right] \tag{4.26}$$

After obtaining the expression for determining the value of constant A in Eq. (4.26) we replace it in Eq. (4.24) to obtain,

$$\bar{\theta}=\frac{1}{\sqrt{s+s^2\tau_q{}^*}}\left[\frac{1}{s}+\tau_q{}^*\right]\left\{\begin{array}{l}\coth\left[\sqrt{s+s^2\tau_q{}^*}\right]\cosh\left[\sqrt{s+s^2\tau_q{}^*}\,\xi\right]-\\ \sinh\left[\sqrt{s+s^2\tau_q{}^*}\,\xi\right]\end{array}\right\} \tag{4.27}$$

$$\bar{\theta} = \frac{1}{\sqrt{s+s^2\tau_q^*}}\left[\frac{1}{s}+\tau_q^*\right]\left\{\frac{\cosh\left[\sqrt{s+s^2\tau_q^*}(1-\xi)\right]}{\sinh\left[\sqrt{s+s^2\tau_q^*}\right]}\right\} \tag{4.28}$$

Subsequently one can also express Eq. (4.28) in exponential form. A result of this demonstration is shown below,

$$\bar{\theta} = \frac{1}{\sqrt{s+s^2\tau_q^*}}\left[\frac{1}{s}+\tau_q^*\right]\left\{\frac{e^{\left[\sqrt{s+s^2\tau_q^*}(1-\xi)\right]}+e^{-\left[\sqrt{s+s^2\tau_q^*}(1-\xi)\right]}}{e^{\left[\sqrt{s+s^2\tau_q^*}\right]}-e^{-\left[\sqrt{s+s^2\tau_q^*}\right]}}\right\} \tag{4.29}$$

$$\bar{\theta} = \frac{1}{\sqrt{s+s^2\tau_q^*}}\left[\frac{1}{s}+\tau_q^*\right]\left\{\frac{e^{-\left[\sqrt{s+s^2\tau_q^*}\,\xi\right]}+e^{-\left[\sqrt{s+s^2\tau_q^*}(2-\xi)\right]}}{1-e^{-2\left[\sqrt{s+s^2\tau_q^*}\right]}}\right\} \tag{4.30}$$

A close observation if Eq. (4.30) will encourage us to comment on the denominator of the term inside the brackets. This form can be expanded in terms of a series using Taylor series expansion method.

Note III: The Taylor series expansion for the expression $\frac{1}{1-\varepsilon}$ *is given by,*

$$\frac{1}{1-\varepsilon} = 1+\varepsilon+\varepsilon^2+\varepsilon^3+\ldots..+\varepsilon^n = \sum_{m=0}^{\infty}\varepsilon^m .$$

Comparing the denominator of the term inside the brackets in Eq. (4.30) with *Note III*, the resulting expression looks like,

$$\bar{\theta} = \frac{1}{\sqrt{s+s^2\tau_q^*}}\left[\frac{1}{s}+\tau_q^*\right]\sum_{m=0}^{\infty}\left\{e^{-\left[\sqrt{s+s^2\tau_q^*}(2m+\xi)\right]}+e^{-\left[\sqrt{s+s^2\tau_q^*}\{2(m+1)-\xi\}\right]}\right\} \tag{4.31}$$

$$\bar{\theta} = \frac{1}{s}\sum_{m=0}^{\infty}\left\{\frac{e^{-\left[\sqrt{s+s^2\tau_q^*}(2m+\xi)\right]} + e^{-\left[\sqrt{s+s^2\tau_q^*}\{2(m+1)-\xi\}\right]}}{\sqrt{s+s^2\tau_q^*}}\right\} +$$

$$\tau_q^*\sum_{m=0}^{\infty}\left\{\frac{e^{-\left[\sqrt{s+s^2\tau_q^*}(2m+\xi)\right]} + e^{-\left[\sqrt{s+s^2\tau_q^*}\{2(m+1)-\xi\}\right]}}{\sqrt{s+s^2\tau_q^*}}\right\} \quad (4.32)$$

$$\bar{\theta} = \frac{1}{\sqrt{\tau_q^*}}\frac{1}{s}\sum_{m=0}^{\infty}\left\{\frac{e^{-(2m+\xi)\sqrt{\tau_q^*}*\left[\sqrt{s(s+\frac{1}{\tau_q^*})}\right]}}{\sqrt{s(s+\frac{1}{\tau_q^*})}} + \frac{e^{-\{2(m+1)-\xi\}\sqrt{\tau_q^*}*\left[\sqrt{s(s+\frac{1}{\tau_q^*})}\right]}}{\sqrt{s(s+\frac{1}{\tau_q^*})}}\right\} +$$

$$\sqrt{\tau_q^*}\sum_{m=0}^{\infty}\left\{\frac{e^{-(2m+\xi)\sqrt{\tau_q^*}*\left[\sqrt{s(s+\frac{1}{\tau_q^*})}\right]}}{\sqrt{s(s+\frac{1}{\tau_q^*})}} + \frac{e^{-\{2(m+1)-\xi\}\sqrt{\tau_q^*}*\left[\sqrt{s(s+\frac{1}{\tau_q^*})}\right]}}{\sqrt{s(s+\frac{1}{\tau_q^*})}}\right\} \quad (4.33)$$

Comparing Eq. (4.33) with *Note II*, one can easily draw similarity between them and thus encourages us to take the Inverse Laplace transform of the obtained equation, Eq. (4.33).

The Inverse Laplace transform will give us the temperature distribution in a finite body using a thermal wave model for dielectric materials.

$$\theta = \frac{1}{\sqrt{\tau_q^*}}\sum_{m=0}^{\infty}\int_{\eta_d}^{\eta_f} e^{-\frac{\eta}{2\sqrt{\tau_q^*}}} I_0\left[\frac{1}{2\sqrt{\tau_q^*}}\sqrt{t^2-\tau_q^*(2m+\xi)^2}\right]d\eta$$

$$+\frac{1}{\sqrt{\tau_q^*}}\sum_{m=0}^{\infty}\int_{\eta_d}^{\eta_f} e^{-\frac{\eta}{2\sqrt{\tau_q^*}}} I_0\left[\frac{1}{2\sqrt{\tau_q^*}}\sqrt{t^2-\tau_q^*\{2(m+1)-\xi\}^2}\right]d\eta$$

$$+\sqrt{\tau_q^*}\sum_{m=0}^{\infty} e^{-\frac{\eta}{2\sqrt{\tau_q^*}}} I_0\left[\frac{1}{2\sqrt{\tau_q^*}}\sqrt{t^2-\tau_q^*(2m+\xi\}^2}\right] \quad (4.34)$$

$$+\sqrt{\tau_q^*}\sum_{m=0}^{\infty} e^{-\frac{\eta}{2\sqrt{\tau_q^*}}} I_0\left[\frac{1}{2\sqrt{\tau_q^*}}\sqrt{t^2-\tau_q^*\{2(m+1)-\xi\}^2}\right]$$

4.3 Thermal Wave in a plate with prescribed temperature on the surface

The governing equation for determining the temperature solution in a plate when it is subjected to a thermal wave is expressed by the same equation used earlier in the study, Eq. (4.1). Following the same procedure that was adopted to solve for the temperature solution in a plate for prescribed heat flux case one can derive the solution for the current case, prescribed temperature. Hence the final form of the thermal wave equation in dimensionless form becomes,

$$\frac{\partial^2\theta}{\partial\xi^2} = \frac{\partial\theta}{\partial\eta} + \tau_q{}^* \frac{\partial^2\theta}{\partial\eta^2} \tag{4.35}$$

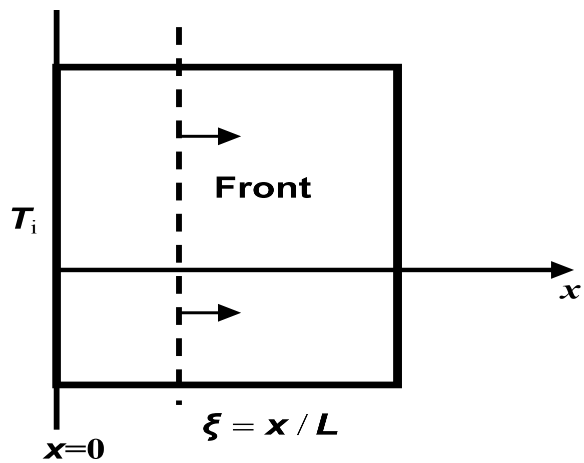

Figure 4.2 Geometry of a flat dielectric plate with prescribed temperature T_0 at the surface x=0

where the dimensionless form of temperature θ is given by $\theta \to \frac{T - T_i}{T_w - T_i}$ and T, T_w and T_i are surface temperature, wall temperature and the initial temperature respectively. The following step is to alter the boundary conditions from the regular form to a dimensionless form. To solve the above differential equation, Eq. (4.35) we need two boundary conditions, one at x = 0 and another one at x = L. The boundary conditions specified at x = 0 is that of a prescribed temperature T_i at time t = 0.

The alternate boundary condition is at x = L where the plate is insulated. Hence there is no heat flow coming in or going out. These boundary conditions can be expressed mathematically in a way shown below.

At x = 0, that is $\xi = 0$ we have T = T_0 and hence based on our selection of boundary condition we can say that

$$\theta\big|_{\xi=0} = \frac{T_0 - T_i}{T_w - T_i} = \theta_0 \tag{4.36}$$

Laplace Transform of Eq. (4.36) would result in,

$$L\{\theta\} = L\{\theta_0\} = \bar{\theta} = \overline{\theta_0} \tag{4.37}$$

A special case would be described as when the prescribed wall temperature T_0 would be equal to the initial temperature of the body T_i. The mathematical formulation is shown below.

$$\theta\big|_{\xi=0} = \frac{T_0 - T_i}{T_0 - T_i} = 1 \tag{4.38}$$

Hence the Laplace transform of Eq. (4.38) would be,

$$L\{\theta\} = L\{1\} = \frac{1}{s} \tag{4.39}$$

At x = L, using boundary condition of second kind, that is q = 0 one deduces the following equations.

$$-k\,\frac{\partial T}{\partial x}\bigg|_{x=L} = 0 \tag{4.40}$$

$$\frac{\partial \theta}{\partial \xi}\bigg|_{\xi=1} = 0 \tag{4.41}$$

By taking Laplace transform of Eq. (4.41),

$$\frac{\partial \bar{\theta}}{\partial \xi}\bigg|_{\xi=1} = 0 \tag{4.42}$$

Taking Laplace transform of the governing equation, Eq. (4.35) we obtain Eq. (4.17) which has been discussed in the earlier case.

$$\frac{\partial^2 \overline{\theta}}{\partial \xi^2} = s\overline{\theta} + s^2 \tau_q^* \overline{\theta} \tag{4.43}$$

Solution to the above equation, Eq. (4.43) can be obtained straight from the case discussed previously with minor alterations and can be used in the present instance to solve the problem.

$$\overline{\theta} = C \cosh\left[\sqrt{s + s^2 \tau_q^*}\,(1-\xi)\right] + D \sinh\left[\sqrt{s + s^2 \tau_q^*}\,(1-\xi)\right] \tag{4.44}$$

Applying the different boundary conditions talked earlier we can derive the values of the constants *C* and *D*. The Eq. (4.37) talks about the first boundary condition and applying it to Eq. (4.44) would help us derive a relation between $\overline{\theta_0}$, *C* and *D*.

$$\overline{\theta_0} = C \cosh\left[\sqrt{s + s^2 \tau_q^*}\,\right] + D \sinh\left[\sqrt{s + s^2 \tau_q^*}\,\right] \tag{4.45}$$

The following step would be to apply the second boundary condition to Eq. (4.42) to Eq. (4.44) to further reduce Eq. (4.45).

$$\left.\frac{\partial \overline{\theta}}{\partial \xi}\right|_{\xi=1} = -C\sqrt{s + s^2 \tau_q^*}\ \sinh\left[\sqrt{s + s^2 \tau_q^*}\,(0)\right] - D\sqrt{s + s^2 \tau_q^*}\ \cosh\left[\sqrt{s + s^2 \tau_q^*}\,(0)\right] \tag{4.46.1}$$

$$0 = -D\sqrt{s + s^2 \tau_q^*} \tag{4.46.2}$$

$$D = 0 \tag{4.47}$$

Substituting the value of *D* obtained in Eq. (4.47) back in Eq. (4.45) to get *C*,

$$C = \frac{\overline{\theta_0}}{\cosh\left[\sqrt{s + s^2 \tau_q^*}\,\right]} \tag{4.48}$$

Replacing Eq. (4.44) with the attained values *C* and *D* we obtain,

$$\overline{\theta} = \frac{\overline{\theta_0}}{\cosh\left[\sqrt{s + s^2 \tau_q^*}\,\right]}\ \cosh\left[\sqrt{s + s^2 \tau_q^*}\,(1-\xi)\right] \tag{4.49}$$

Subsequently one can also express Eq. (4.49) in exponential form. A result of this demonstration is shown below,

$$\overline{\theta} = \overline{\theta_0} \left\{ \frac{e^{\left[\sqrt{s+s^2\tau_q^*}(1-\xi)\right]} + e^{-\left[\sqrt{s+s^2\tau_q^*}(1-\xi)\right]}}{e^{\left[\sqrt{s+s^2\tau_q^*}\right]} + e^{-\left[\sqrt{s+s^2\tau_q^*}\right]}} \right\} \tag{4.50}$$

$$\overline{\theta} = \overline{\theta_0} \left\{ \frac{e^{-\left[\sqrt{s+s^2\tau_q^*}\ \xi\right]} + e^{-\left[\sqrt{s+s^2\tau_q^*}\ (2-\xi)\right]}}{1+e^{-2\left[\sqrt{s+s^2\tau_q^*}\right]}} \right\} \tag{4.51}$$

Note IV: The Taylor series expansion for the expression $\frac{1}{1+\varepsilon}$ *is given by,*

$$\frac{1}{1+\varepsilon} = 1-\varepsilon+\varepsilon^2-\varepsilon^3+\ldots..+(-1)^n\ \varepsilon^n = \sum_{m=0}^{\infty}(-1)^m\ \varepsilon^m$$

Relating the denominator of the term inside the brackets in Eq. (4.51) with *Note IV*, the resulting expression looks like,

$$\overline{\theta} = \overline{\theta_0}\ \sum_{m=0}^{\infty}\ (-1)^m \left\{ e^{-2m\left[\sqrt{s+s^2\tau_q^*}\right]} \left(e^{-\left[\sqrt{s+s^2\tau_q^*}\ \xi\right]} + e^{-\left[\sqrt{s+s^2\tau_q^*}\ (2-\xi)\right]} \right) \right\} \tag{4.52}$$

$$\overline{\theta} = \overline{\theta_0}\ \sum_{m=0}^{\infty}\ (-1)^m \left\{ e^{-\sqrt{s+s^2\tau_q^*}\ (2m+\xi)} + e^{-\sqrt{s+s^2\tau_q^*}\ [2(m+1)-\xi]} \right\} \tag{4.53}$$

Recall, the inverse Laplace transforms of Eq. (4.53) is obtainable using a technique discussed in [17] as shown in Eq. (2.6.1)

$$L^{-1}\left\{\exp\left[-\sqrt{s(s+1)}\ \xi\right]\right\} = \exp\left[-\frac{\eta}{2}\right] \times \left\{ \delta\left[\eta-\xi\right] + H(\xi-\eta)\frac{\xi}{2}\ \frac{I_1\left[\frac{1}{2}\sqrt{\eta^2-\xi^2}\right]}{\sqrt{\eta^2-\xi^2}} \right\}$$

Thus the temperature solution is given by the following relation,

$$\theta = \sum_{m=0}^{\infty} (-1)^m \left\{ \begin{aligned} &\exp\left[-\frac{\varphi_1}{2}\right] H[\eta - \varphi_1] + \frac{\varphi_1}{2} \int_{\varphi_1}^{\eta} \frac{e^{-\eta/2}\, I_1\left[\frac{1}{2}\sqrt{\eta^2 - \varphi_1{}^2}\right]}{\sqrt{\eta^2 - \varphi_1{}^2}}\, d\eta \\ &+ \exp\left[-\frac{\varphi_2}{2}\right] H[\eta - \varphi_2] + \frac{\varphi_2}{2} \int_{\varphi_2}^{\eta} \frac{e^{-\eta/2}\, I_1\left[\frac{1}{2}\sqrt{\eta^2 - \varphi_2{}^2}\right]}{\sqrt{\eta^2 - \varphi_2{}^2}}\, d\eta \end{aligned} \right\} \quad (4.54)$$

where φ_1 and φ_2 are given by the relations, $\varphi_1 = \dfrac{2m+\xi}{\sqrt{\tau_q{}^*}}$ and $\varphi_2 = \dfrac{2(m+1)-\xi}{\sqrt{\tau_q{}^*}}$.

4.4 Conclusion

In this chapter flat plate with insignificant thickness was analyzed by applying boundary conditions of first and second kind on either ends of the plate. They are given by Eq. (4.54) and Eq. (4.34) in the chapter. For the second time it has been well demonstrated in this chapter how the classical method of Laplace transform was used to derive an analytical form of the temperature solution so efficiently. The formulated equations are now going to be used to predict the temperature field in the dielectric substance. The analysis of these equations will be done in the following chapter and the thermal behavior will be discussed in detail with the help of several illustrations and data of several cases.

CHAPTER 5

ANALYSIS OF TEMPERATURE DISTRIBUTION DUE TO THE OCCURENCE OF A THERMAL WAVE IN A PLATE

5.1 Introduction

In this chapter we are going to examine the thermal behavior of a flat thin plate of a dielectric material, when it is subjected to different boundary conditions as discussed in the previous chapter. As the mathematical formulation was presented and analytical solutions were obtained prior to this section, we have used them to develop several Mathematica subroutines that are presented in Appendix B of the work. The Eq. (4.34) and Eq. (4.54) have been restricted with finite number of terms to get a good convergence which is very critical in this problem.

The first sub-section shows the variation in temperature distribution in dimensionless space (ξ) holding the dimensionless time (η) constant. Thus for different values of η several temperature profiles for the case, temperature prescribed on the surface of a dielectric finite body are well illustrated in this chapter. The subsequent part essentially focuses on the case when heat flux has been specified on the surface of the dielectric material. The results of which have been well illustrated with the help of graphs and tables.

Also the similarity in the temperature solution of a finite body with that of a semi-infinite body has been emphasized for all times before the wave front strikes the insulated wall. Furthermore special attention has been given to the analysis in a region close to the insulated. wall when the front is just about to strike the surface and when reflection occurs from the surface Certain anomalies have been encountered and an attempt has been taken to explain the cause for the occurrence of those anomalies.

5.2 Analysis of thermal behavior of a dielectric plate for X22 case

Table 5.1 Dimensionless temperature in a plate for a specified dimensionless time under the influence of a heat flux when the wave propagates from x =0 to x = L.

ξ	η = 0.2	η = 0.6	η = 1.0
	θ	θ	θ
0	1.09758	0.111788	0.102719
0.02	1.07765	0.111786	0.102716
0.04	1.05787	0.111778	0.102709
0.06	1.03823	0.111765	0.102698
0.08	1.01874	0.111746	0.102682
0.1	0.999395	0.111723	0.102661
0.12	0.980194	0.111694	0.102636
0.14	0.961137	0.11166	0.102606
0.16	0.942226	0.11162	0.102572
0.18	0.923459	0.111576	0.102533
0.2	0.904837	0.111526	0.10249
0.22	0	0.11141	0.102389
0.24	0	0.111344	0.102332
0.26	0	0.111274	0.10227
0.28	0	0.111198	0.102204
0.3	0	0.111116	0.102133
0.32	0	0.11103	0.102058
0.34	0	0.950442	0.101978
0.36	0	0.941651	0.101893
0.38	0	0.924171	0.101804
0.4	0	0.906827	0.101711
0.42	0	0.889618	0.101613
0.44	0	0.872545	0.10151
0.46	0	0.855607	0.101403
0.48	0	0.838804	0.101292
0.5	0	0.822137	0.101176
0.54	0	0.789205	0.100931
0.58	0	0.756813	0.100667
0.6	0	0.740818	0.100529
0.7	0	0	0.099772
0.8	0	0	0.749196
0.9	0	0	0.67631
1	0	0	0.606531

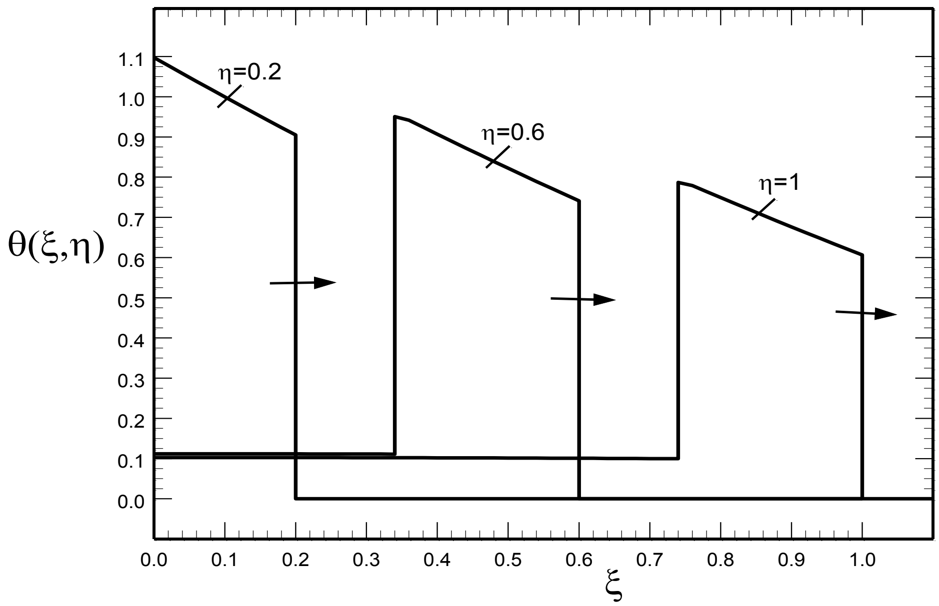

Figure 5.1 Dimensionless temperature distribution in a flat thin dielectric plate at different dimensionless time when wave propagates from $x = 0$ to $x = L$.

Table 5.2 Dimensionless temperature in a flat plate for a specified dimensionless time under the influence of a heat flux when the wave reflects backward after striking the insulated wall.

ξ	***η* = 1.0**	***η* = 1.1**	***η* = 1.2**
	θ	***θ***	***θ***
0	0.166936	0.163586	0.160383
0.01	0.166935	0.163585	0.160382
0.02	0.166932	0.163583	0.160379
0.03	0.166927	0.163578	0.160375
0.04	0.166921	0.163572	0.160369
0.05	0.166912	0.163564	0.160361
0.06	0.166902	0.163554	0.160351
0.07	0.16689	0.163542	0.16034
0.08	0.166876	0.163528	0.160326
0.09	0.16686	0.163513	0.160311
0.1	0.166842	0.163495	0.160295
0.11	0.166822	0.163476	0.160276
0.12	0.1668	0.163455	0.160256
0.13	0.166777	0.163433	0.160234
0.14	0.166751	0.163408	0.16021
0.15	0.166724	0.163382	0.160185

Table 5.2 – continued

ξ	η = 1.0	η = 1.1	η = 1.2
	θ	θ	θ
0.16	0.166695	0.163354	0.160158
0.17	0.166664	0.163324	0.160129
0.18	0.166631	0.163292	0.160098
0.19	0.166596	0.163258	0.160065
0.2	0.16656	0.163223	0.160031
0.21	0.166521	0.163186	0.159995
0.22	0.166481	0.163147	0.159957
0.23	0.166439	0.163106	0.159918
0.24	0.166394	0.163063	0.159876
0.25	0.166348	0.163018	0.159833
0.26	0.166301	0.162972	0.159789
0.27	0.166251	0.162924	0.159742
0.28	0.166199	0.162874	0.159694
0.29	0.166146	0.162822	0.159644
0.3	0.16609	0.162769	0.159592
0.31	0.166033	0.162714	0.159538
0.32	0.165974	0.162656	0.159483
0.33	0.165913	0.162598	0.159426
0.34	0.16585	0.162537	0.159367
0.35	0.165786	0.162474	0.159307
0.36	0.165719	0.16241	0.159245
0.37	0.165651	0.162344	0.159181
0.38	0.16558	0.162276	0.159115
0.39	0.165508	0.162206	0.159048
0.4	0.165434	0.162135	0.158978
0.41	0.165359	0.162061	0.158908
0.42	0.165281	0.161986	0.158835
0.43	0.165201	0.161909	0.15876
0.44	0.16512	0.161831	0.158684
0.45	0.165037	0.16175	0.158607
0.46	0.164952	0.161668	0.158527
0.47	0.164865	0.161584	0.158446
0.48	0.164776	0.161498	0.158363
0.49	0.164685	0.161411	0.158278
0.5	0.164593	0.161321	0.158191
0.51	0.164499	0.16123	0.158103
0.52	0.164403	0.161137	0.158013
0.53	0.164305	0.161042	0.157922
0.54	0.164205	0.160946	0.157828
0.55	0.164103	0.160848	0.157733
0.56	0.164	0.160748	0.157637
0.57	0.163894	0.160646	0.157538
0.58	0.163787	0.160542	0.157438
0.59	0.163678	0.160437	0.157336
0.6	0.904386	0.16033	0.157233

Table 5.2 – continued

ξ	*η* = 1.0	*η* = 1.1	*η* = 1.2
	θ	*θ*	*θ*
0.61	0.896326	0.160221	0.157127
0.62	0.888298	0.16011	0.15702
0.63	0.880302	0.159998	0.156912
0.64	0.872338	0.159884	0.156801
0.65	0.864405	0.159768	0.156689
0.66	0.856504	0.15965	0.156575
0.67	0.848634	0.159531	0.15646
0.68	0.840796	0.15941	0.156343
0.69	0.832989	0.159287	0.156224
0.7	0.825215	0.863851	0.156103
0.71	0.817471	0.856077	0.155981
0.72	0.809759	0.848335	0.155857
0.73	0.802079	0.840624	0.155732
0.74	0.79443	0.832943	0.155604
0.75	0.786813	0.825294	0.155475
0.8	0.749196	0.787514	1.37394
0.9	0.67631	1.29122	1.36493
1	1.21306	1.28818	1.36193

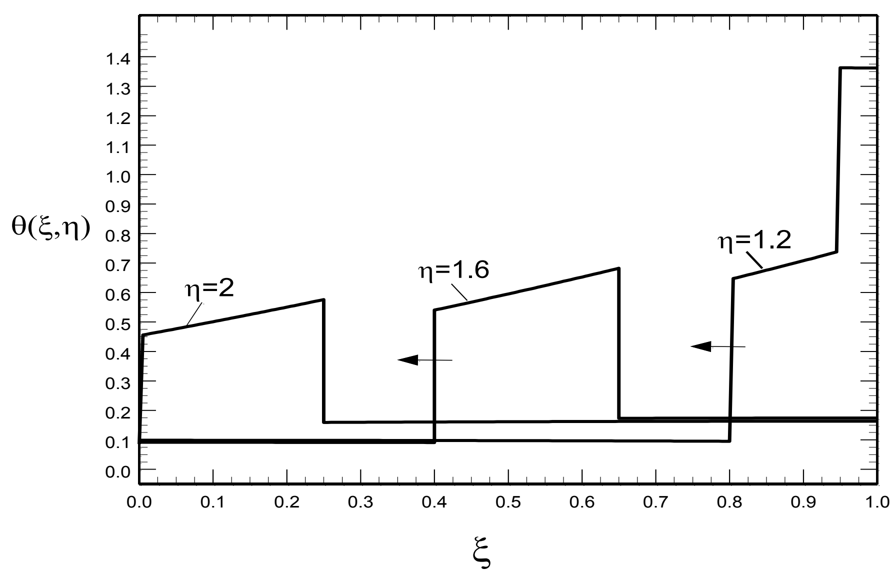

Figure 5.2 Reflection of a heat wave after the front strikes the insulated wall for $\eta \geq 1$

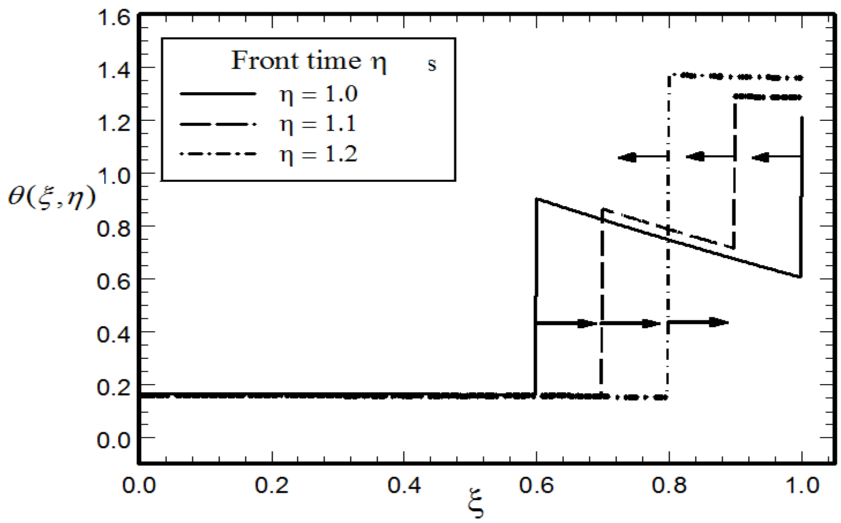

Figure 5.3 Propagation and reflection effect of a thermal wave in a finite body.

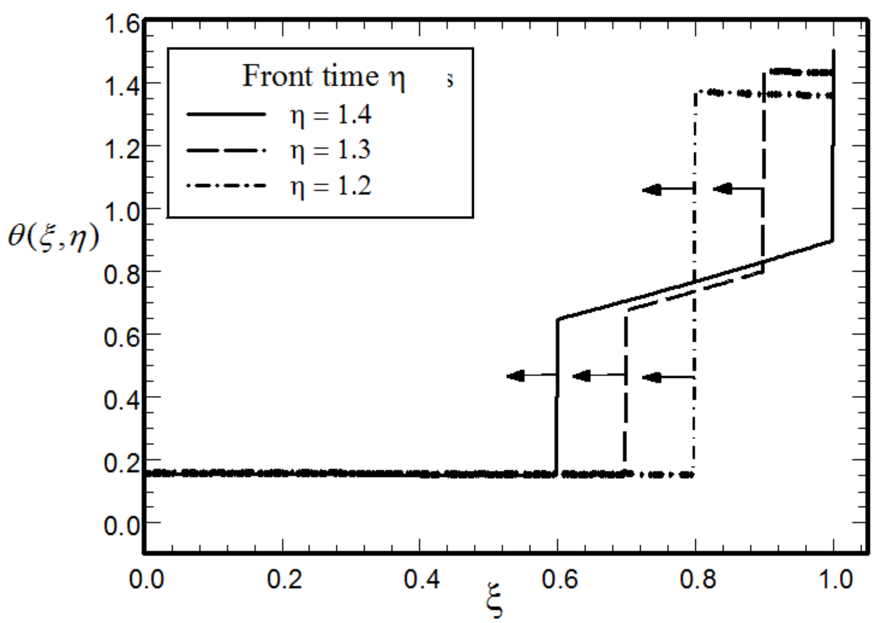

Figure 5.4 Front reflecting back of an insulated wall for dimensionless time $\eta = 1.2, 1.3$ and 1.4

Here we are analyzing the case of prescribed heat flux at the surface $x = 0$ for a flat thin plate which is insulated at the other end, $x = L$. The equation to calculate the dimensionless temperature variable θ is given by Eq. (4.34) which was formulated using the classical Laplace transformation. For convenience of the reader let us recall the equation over here which will help us make some critical observation of the solution.

$$
\begin{aligned}
\theta = {} & \frac{1}{\sqrt{\tau_q{}^*}} \sum_{m=0}^{\infty} \int_{\eta_d}^{\eta_f} e^{-\frac{\eta}{2\sqrt{\tau_q{}^*}}} I_0\left[\frac{1}{2\sqrt{\tau_q{}^*}}\sqrt{t^2 - \tau_q{}^*(2m+\xi)^2}\right] d\eta \\
& + \frac{1}{\sqrt{\tau_q{}^*}} \sum_{m=0}^{\infty} \int_{\eta_d}^{\eta_f} e^{-\frac{\eta}{2\sqrt{\tau_q{}^*}}} I_0\left[\frac{1}{2\sqrt{\tau_q{}^*}}\sqrt{t^2 - \tau_q{}^*\{2(m+1)-\xi\}^2}\right] d\eta \\
& + \sqrt{\tau_q{}^*} \sum_{m=0}^{\infty} e^{-\frac{\eta}{2\sqrt{\tau_q{}^*}}} I_0\left[\frac{1}{2\sqrt{\tau_q{}^*}}\sqrt{t^2 - \tau_q{}^*(2m+\xi\}^2}\right] \\
& + \sqrt{\tau_q{}^*} \sum_{m=0}^{\infty} e^{-\frac{\eta}{2\sqrt{\tau_q{}^*}}} I_0\left[\frac{1}{2\sqrt{\tau_q{}^*}}\sqrt{t^2 - \tau_q{}^*\{2(m+1)-\xi\}^2}\right]
\end{aligned}
\tag{4.34}
$$

To perform an analysis we have restricted ourselves to consider finite number of terms for the series in Eq. (4.34).This has been done because there is no change in the temperature profile for any value of $m > \eta$ and also to get a better convergence. It also reduces the computation time significantly. For instance when $m = 0$ in the equation all the terms are left only with ξ which means that the front can only travel the length of the plate for once and thus the effect of reflection if time is greater than 1, that is, $\eta > 1$ cannot be observed. In most of the cases discussed here in this work we have restricted the value of m to be as 4.

The Table 5.1 represents the value of non-dimensional temperature (θ) at different non-dimensional time (η) in a finite non-dimensional space (ξ). An observation of the table will help us realize that we have initially analyzed the part where the wave propagates form the surface $x = 0$ to the insulated wall $x = L$. Non-dimensional temperature solutions that are obtained at every non-dimensional time of $\eta < 1$ as a result of a propagating heat wave were similar to the results that were previously obtained for a semi-infinite body maintaining the same boundary condition at *x* = 0. When a unit pulse of heat is applied on the surface of the plate, the heat does not start penetrating through the surface immediately which thus gives rise to the phenomena of hyperbolic heat conduction. Instead it slowly builds up and then a pulse is generated in some specified time at a particular location inside the body. This pulse then travels inside the body of finite length before it reaches the other end with finite speed. The front that is moving with a speed (σ) given by the ratio of thermal diffusivity (α) and the square of the lag time due to heat flux (τ_q), that is, the mathematical representation is given by $\sigma = \sqrt{\alpha/\tau_q}$ [13]. An illustration of this process is shown in Figure 5.1 which was generated after solving the Eq. (4.34) for values of $\eta \leq 1$ some of which are presented in tabular form in Table 5.1.

Subsequently we are going to look at what happens when the wave reflects back of the insulated wall. This is a salient feature of the problem and hence more emphasis has been given to its analysis by viewing the eccentric thermal behaviors occurring in an area of close proximity to the insulated surface. When the pulse that was travelling with a finite speed of σ in the plate comes in contact with the insulated surface at *x* = *L*, the surface starts reflecting the thermal energy induced by the pulse. Hence the temperature of the surface at *x* = *L* increases significantly and it starts reflecting back heat waves. Analysis has shown us that there is an abrupt jump in temperature in a space which is located very close to the wall surface, refer Figure 5.2. The cause behind this abrupt jump in temperature is explained in this study with help of phonons vibrating in a very small space as a result of which the kinetic energy gets converted into thermal energy. The work presented in this thesis essentially deals with sub-micron geometry dielectric material when heated rapidly in a very small time of like nanoseconds to picoseconds. Thus a crystalline state of the material can be brought into consideration to describe the cause of the sudden jump in temperature.

A phonon in quantum physics is defined to be a vibration when a lattice oscillates uniformly at the same frequency. The density of states is defined as the number of states at each energy level left to be occupied by electrons. In thermodynamics the phonon density of states determines the specific heat capacity of the crystal. The energy of phonon fluctuates between some mean values when it is in excited state. Now referring to Figure 5.2 we can see this temperature rise taking place in very small space. At a dimensionless time slightly over one, that is, $\eta = 1^{+}$, the temperature inside the body shoots up to a value between 1.21306 to 1.36193. These values are obtained from Table 5.2 of the study. Notice from Table 5.1 the value of non-dimensional temperature was 0.606531 when the first front struck the surface. After subsequent fronts have struck the surface as time passed by we have seen the temperature at the surface buildup to a value of 1.21306 which is a jump by 49.99%, approximately twice the previous obtained value when the first set of wave fronts travelled the entire span of the body. This is a significant jump which encouraged us to go further in detail and understand the cause behind it. A sample math formulation based on fundamental theory was considered to be the best possible explanation in view of the context of this study. The discussion is presented with the help of Figure 5.5 as shown below,

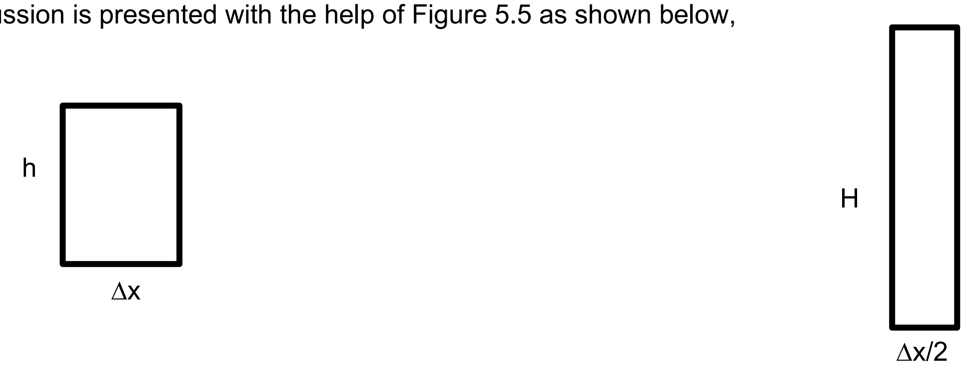

(a) (b)

Figure 5.5 Representation of phonon excitation levels in a region inside the plate (a) at normal state (b) when it has reached an excited state.

Let us begin by considering the Figure 5.5 (a) where we assume the total energy present in the body be U. Mathematically one can express the following set of equations. They are given by a simple relation that states energy inside the body sown in Figure 5.5 (a) is equal to the product of the number of phonons with the energy of each phonon. This is expressed as,

$$\rho\,.\Delta x.1.C.T = N_{phonon} \times e_{phonon} \tag{5.1}$$

$$.T = \frac{N_{phonon} \times e_{phonon}}{\rho\,.\Delta x.1.C} \tag{5.2}$$

where ρ is the density of the material in *kg/ m*^{3} , $(\Delta x.1)$ is the volume in *m*^{3} , C is the specific heat of the material in *J/ kg K*, *T* is the temperature in *K* , N_{phonon} is the number of phonons and e_{phonon} is equal to energy of each phonon ($e_{phonon} = h\,\nu$). All other parameters will remain constant except for Δx which we specify to be as half the initial specified value. The geometry of the problem is shown in Figure 5.5 (b). Thus the energy stored in the body represented by Figure 5.5 (a) will be the same and thus if you replace Δx by $\Delta x\,/2$, the dimensionless temperature rises by a factor of two.

$$.T = \frac{N_{phonon} \times e_{phonon}}{\rho\,.(\Delta x/2).1.C} \tag{5.3}$$

$$.T_{new} = 2\,T = \frac{N_{phonon} \times e_{phonon}}{\rho\,\Delta x.1.C} \tag{5.4}$$

where T_{new} is the newly obtained temperature of the body due to vibration of phonons. This jump has been well illustrated with the help of Figure 5.3 and 5.4 in the study. Figure 5.3 also shows the superposition of a propagating and reflecting heat waves of different amplitudes at a location closer to the insulated wall. From Figure 5.2 and 5.4 one can comment that the pulse retains back to its standard profile for a larger non-dimensional time η of 1.4 onwards.

5.3 Analysis of thermal behavior of a dielectric plate for X12 case

Table 5.3 Dimensionless temperature in a flat plate for specified dimensionless time with constant wall temperature when the wave propagates from *x* =0 to *x* = *L*.

ξ	η = 0.2	η = 0.4	η = 0.6	η = 0.8	η = 1.0
	θ	θ	θ	θ	θ
0	1	1	1	1	1
0.02	0.990476	0.990908	0.9913	0.991658	0.991985
0.04	0.980953	0.981816	0.982601	0.983317	0.983971
0.06	0.97143	0.972725	0.973903	0.974977	0.975958

Table 5.3 – continued

ξ	η = 0.2	η = 0.4	η = 0.6	η = 0.8	η = 1.0
	θ	θ	θ	θ	θ
0.08	0.961909	0.963636	0.965206	0.966637	0.967946
0.1	0.95239	0.954548	0.95651	0.9583	0.959935
0.12	0.942873	0.945462	0.947817	0.949964	0.951925
0.14	0.933359	0.936379	0.939126	0.94163	0.943918
0.16	0.923848	0.927299	0.930438	0.933299	0.935914
0.18	0.91434	0.918223	0.921753	0.924971	0.927912
0.2	0	0.90915	0.913071	0.916646	0.919913
0.22	0	0.900081	0.904394	0.908325	0.911918
0.24	0	0.891018	0.895721	0.900008	0.903926
0.26	0	0.881959	0.887053	0.891696	0.895939
0.28	0	0.872906	0.87839	0.883389	0.887957
0.3	0	0.86386	0.869733	0.875086	0.879979
0.32	0	0.854819	0.861081	0.86679	0.872007
0.34	0	0.845786	0.852436	0.858499	0.86404
0.36	0	0.836759	0.843798	0.850215	0.856079
0.38	0	0.827741	0.835168	0.841938	0.848125
0.4	0	0	0.826544	0.833667	0.840177
0.42	0	0	0.817929	0.825405	0.832236
0.44	0	0	0.809322	0.817149	0.824302
0.46	0	0	0.800724	0.808903	0.816377
0.48	0	0	0.792136	0.800665	0.808459
0.5	0	0	0.783556	0.792435	0.800549
0.52	0	0	0.774987	0.784215	0.792649
0.54	0	0	0.766428	0.776005	0.784757
0.56	0	0	0.75788	0.767805	0.776875
0.58	0	0	0.749344	0.759615	0.769002
0.6	0	0	0	0.751436	0.76114
0.62	0	0	0	0.743269	0.753288
0.64	0	0	0	0.735112	0.745447
0.66	0	0	0	0.726968	0.737617
0.68	0	0	0	0.718836	0.729798
0.7	0	0	0	0.710716	0.721991
0.72	0	0	0	0.70261	0.714197
0.74	0	0	0	0.694516	0.706415
0.76	0	0	0	0.686437	0.698645
0.78	0	0	0	0.678371	0.690889
0.8	0	0	0	0	0.683146
0.82	0	0	0	0	0.675417
0.84	0	0	0	0	0.667702
0.86	0	0	0	0	0.660002
0.88	0	0	0	0	0.652316
0.9	0	0	0	0	0.644645
0.94	0	0	0	0	0.629351
0.98	0	0	0	0	0.614121
1	0	0	0	0	0

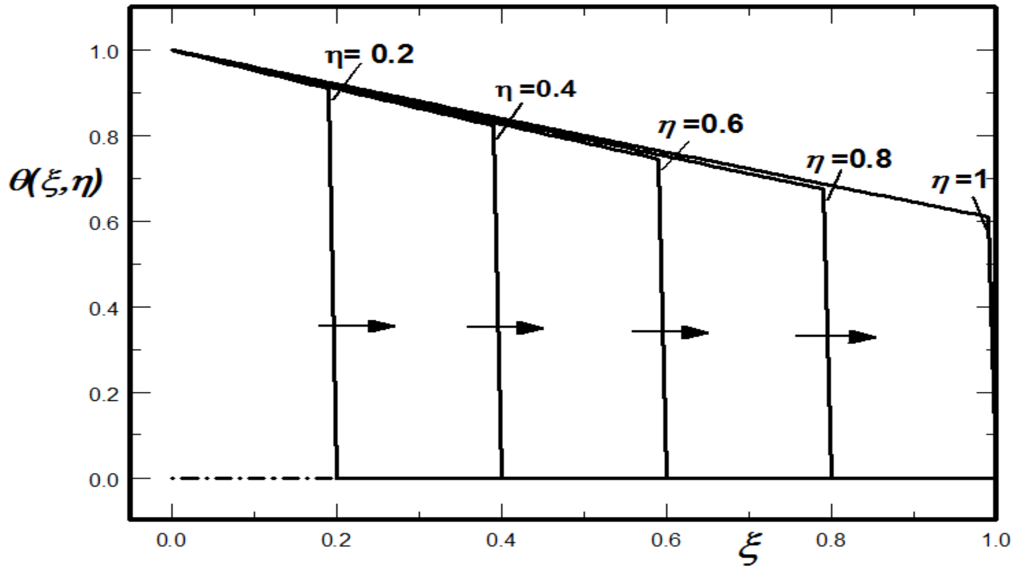

Figure 5.6 Dimensionless temperature distribution in a flat thin dielectric plate at different dimensionless times when wave propagates from x = 0 to x = L for X12 case.

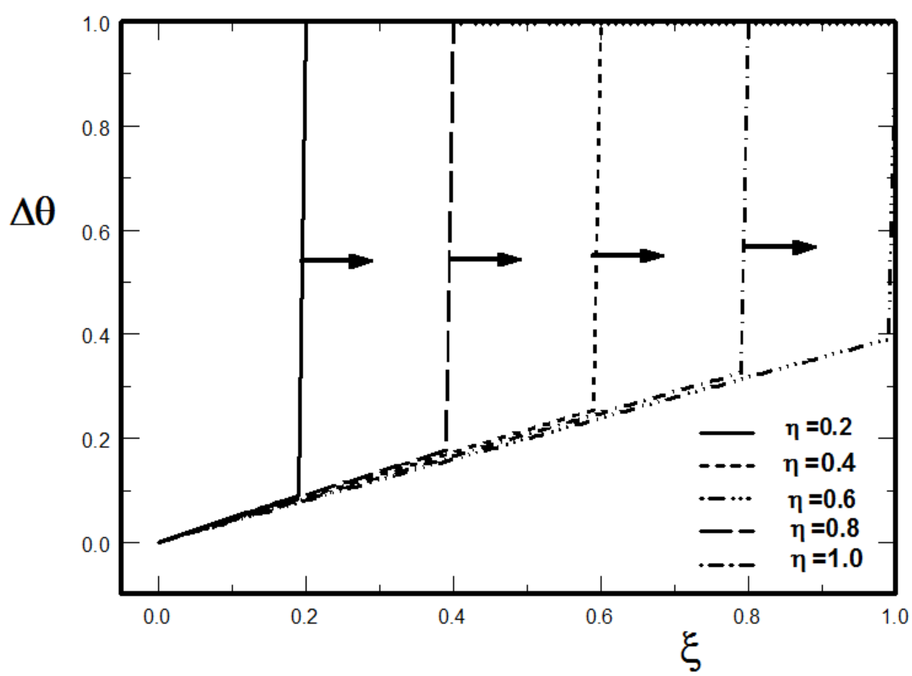

Figure 5.7 Front moving forward for different values of dimensionless time when x = 0 to x = L for X12 case.

After analyzing the X22 case we are now going to perform the analysis for X12 case, that is when constant wall temperature is prescribed at *x* = 0 and insulated wall at *x* = *L*. The analysis was done by solving the Eq. (4.54) for finite number of terms to get a better convergence. The equation has been presented again in this chapter for the convenience of the reader.

$$\theta = \sum_{m=0}^{\infty} (-1)^m \left\{ \begin{aligned} &\exp\left[-\frac{\varphi_1}{2}\right] H[\eta-\varphi_1] + \frac{\varphi_1}{2} \int_{\varphi_1}^{\eta} \frac{e^{-\eta/2}\, I_1\left[\frac{1}{2}\sqrt{\eta^2-\varphi_1{}^2}\right]}{\sqrt{\eta^2-\varphi_1{}^2}}\, d\eta \\ &+ \exp\left[-\frac{\varphi_2}{2}\right] H[\eta-\varphi_2] + \frac{\varphi_2}{2} \int_{\varphi_2}^{\eta} \frac{e^{-\eta/2}\, I_1\left[\frac{1}{2}\sqrt{\eta^2-\varphi_2{}^2}\right]}{\sqrt{\eta^2-\varphi_2{}^2}}\, d\eta \end{aligned} \right\} \quad (4.54)$$

where, φ_1 and φ_2 are given by the relations, $\varphi_1 = \dfrac{2m+\xi}{\sqrt{\tau_q{}^*}}$ and $\varphi_2 = \dfrac{2(m+1)-\xi}{\sqrt{\tau_q{}^*}}$.

Table 5.2 represents the value of non-dimensional temperature (θ) at different non-dimensional time (η) in a finite non-dimensional space (ξ). In this problem the surface at *x* = 0 is rapidly heated to reach a dimensionless temperature value of one, that is, $\dfrac{\theta}{\theta_0} = 1$. As the surface temperature changes rapidly there is a gradient formed which is noticeable in Figure 5.5 of this chapter. Several different dimensionless temperature profiles are plotted for all dimensionless time of $\eta \leq 1$ and looking at them one can comment on the temperature gradient being fairly uniform. The figure also shows the front moving towards the other end at *x* = *L* of the body where it is going to encounter an insulated wall. Similar results were observed on comparing the results with the results that were obtained for a semi-infinite body for X12 case for all dimensionless time when the front has not encountered the insulated wall and is travelling with a finite speed of (σ) inside the body. In addition to that both Figure 5.6 and Figure 5.7 have a very strong resemblance with the graphical representation shown in [14]. The heat coming in the body is fairly constant because the gradient does not shift by much. Figure

5.7 was plotted by taking the data obtained by taking the difference between the two subsequent non-dimensional temperatures at a specified time interval in the body. The accuracy in these results was very high because they were compared with the work presented in [14] where the investigators have used the Fourier series approach and Green's Function solution to solve the problem. The results obtained here are in close agreement with the results that are presented in [14].

The analysis presented above is followed by examining the behavior of the reflecting wave in a similar way as it was done earlier for the X22 case. Certain anomalies have been encountered while performing the analysis and sincere efforts have been taken to justify their causes and effects.

Table 5.4 Dimensionless temperature in a flat plate for specified dimensionless time with constant wall temperature when the wave propagates from *x* =0 to *x* = *L*.

ξ	η = 1.2		η = 1.4		η = 1.6	
	θ	Δ θ =1- θ	θ	Δ θ =1- θ	θ	Δ θ =1- θ
0	1	0	1	0	1	0
0.02	0.992285	0.007715	0.99256	0.00744	0.992814	0.007186
0.04	0.984571	0.015429	0.985121	0.014879	0.985627	0.014373
0.06	0.976857	0.023143	0.977682	0.022318	0.978442	0.021558
0.08	0.969144	0.030856	0.970244	0.029756	0.971257	0.028743
0.1	0.961432	0.038568	0.962808	0.037192	0.964074	0.035926
0.12	0.953722	0.046278	0.955373	0.044627	0.956892	0.043108
0.14	0.946014	0.053986	0.947939	0.052061	0.949711	0.050289
0.16	0.938309	0.061691	0.940508	0.059492	0.942533	0.057467
0.18	0.930606	0.069394	0.93308	0.06692	0.935357	0.064643
0.2	0.922906	0.077094	0.925654	0.074346	0.928184	0.071816
0.22	0.915209	0.084791	0.918231	0.081769	0.921013	0.078987
0.24	0.907516	0.092484	0.910812	0.089188	0.913846	0.086154
0.26	0.899827	0.100173	0.903396	0.096604	0.906682	0.093318
0.28	0.892142	0.107858	0.895985	0.104015	0.899522	0.100478
0.3	0.884461	0.115539	0.888577	0.111423	0.892366	0.107634
0.32	0.876786	0.123214	0.881175	0.118825	0.885215	0.114785
0.34	0.869116	0.130884	0.873777	0.126223	0.878068	0.121932
0.36	0.861451	0.138549	0.866384	0.133616	0.870925	0.129075
0.38	0.853793	0.146207	0.858998	0.141002	0.863789	0.136211
0.4	0.84614	0.15386	0.851616	0.148384	0.856657	0.143343
0.42	0.838494	0.161506	0.844241	0.155759	1.30516	-0.30516

Table 5.4 – continued

ξ	η = 1.2		η = 1.4		η = 1.6	
	θ	Δ θ =1- θ	θ	Δ θ =1- θ	θ	Δ θ =1- θ
0.44	0.830855	0.169145	0.836873	0.163127	1.30437	-0.30437
0.46	0.823224	0.176776	0.829511	0.170489	1.3036	-0.3036
0.48	0.815599	0.184401	0.822157	0.177843	1.30285	-0.30285
0.5	0.807983	0.192017	0.814809	0.185191	1.30214	-0.30214
0.54	0.792775	0.207225	0.800138	0.199862	1.30079	-0.30079
0.58	0.777602	0.222398	0.7855	0.2145	1.29956	-0.29956
0.6	0.77003	0.22997	0.778194	0.221806	1.29898	-0.29898
0.64	0.754915	0.245085	1.27364	-0.27364	1.29792	-0.29792
0.68	0.739842	0.260158	1.27263	-0.27263	1.29696	-0.29696
0.7	0.732321	0.267679	1.27216	-0.27216	1.29652	-0.29652
0.8	0.694897	0.305103	1.27029	-0.27029	1.29476	-0.29476
0.9	1.24251	-0.24251	1.26917	-0.26916	1.29371	-0.2937
1	1.24211	-0.24211	1.26879	-0.26879	1.29335	-0.29335

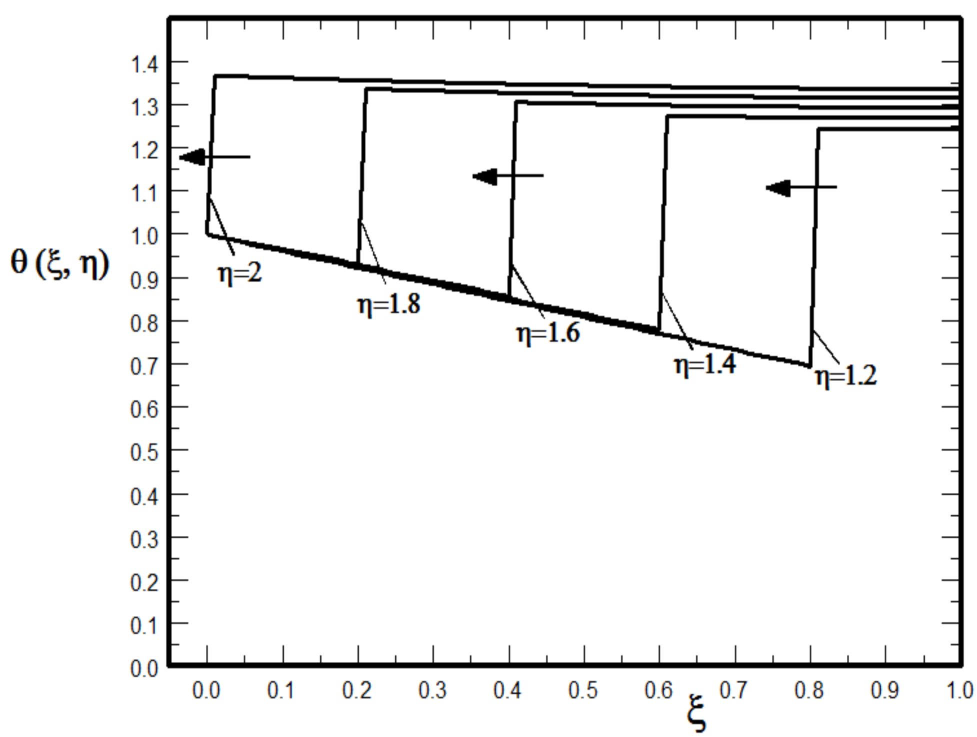

Figure 5.8 Dimensionless temperature distributions in a flat thin dielectric plate at different dimensionless time when wave reflects back of the insulated wall for X12 case.

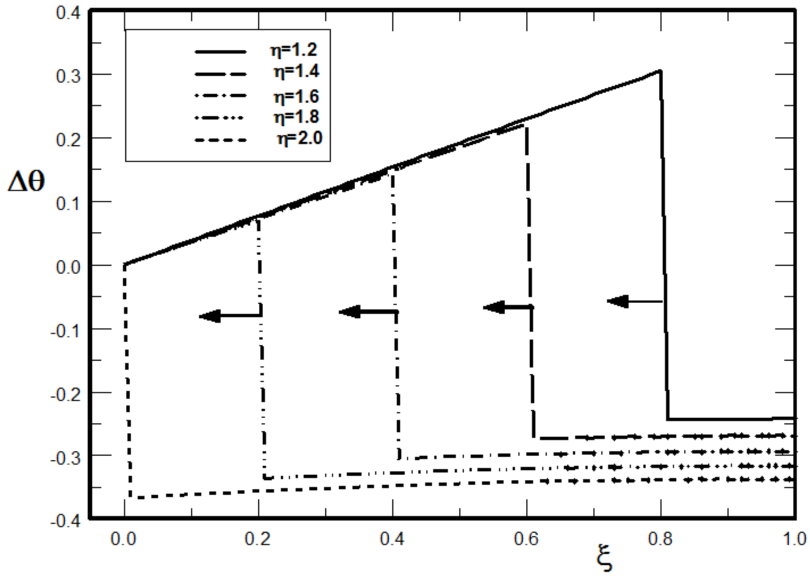

Figure 5.9 Front travelling back in a flat thin dielectric plate at different dimensionless time when wave reflects back of the insulated wall for X12 case.

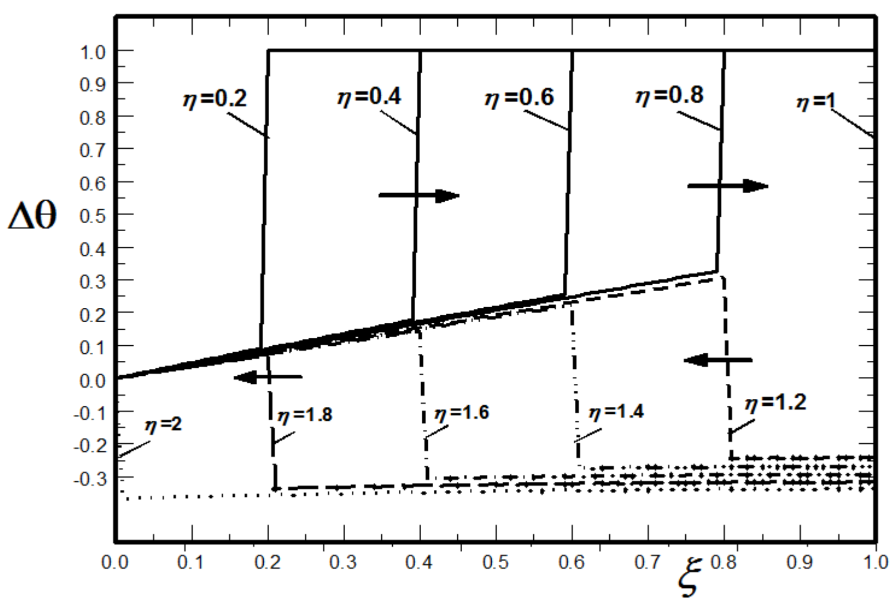

Figure 5.10 Propagation and reflection of a moving front of an insulated wall showing the effect of superposition.

The thermal wave in a dielectric material of fnite size as shown in Figure 5.6 comes in contact with the insulated wall at $x = L$, the energy genarated inside the body due to the propagation of the pulse is being absorbed by the wall. Thus the wall temperature starts rising up and for any non-dimensional time of $\eta > 1$ we see that there is a wave reflecting back of the surface travelling towards the surface at $x = 0$ as shown in Figure 5.8 and Figure 5.9. A careful observation of Figure 5.8 would display that the non-dimensionless temperature goes above the specified value of 1. This strange behaviour has been explained with the excitation level of phonons present in the lattice of the dielectric material and also with theory of superposition of a propagating and reflecting heat wave. The phenomena of superposition has been illustrated in Figure 5.10 in which the solid lines (when $\eta \leq 1$) represent the wave propagation and the dashed lines (when $\eta \geq 1$) represent the reflection of the wall surface.

Observing Figure 5.8 we can say that there is a temperature gradient between $\xi = 0$ and $\xi = 0.8$ for a dimensionless time of $\eta = 1.2$. Also there is drop in temperature when $\eta = \xi$. So for a dimensionless time of 1.2 the value of ξ becomes 0.8 because the front travels the entire span of the plate, that is, from $\xi = 0$ to $\xi = 1$ and then travels two units backwards from $\xi = 1$ to $\xi = 0.8$. The drop in non-dimensional temperature is from 1.24211 units to 0.694897 units. But then as stated earlier that there exists a gradient which in other words say that there is heat coming in. Thus when these two waves encounter each other as shown in Figure 5.10 for $\eta = 0.8$ and $\eta = 1.2$ at the same location of $\xi = 0.8$ they superimpose with each other. The result of which is observed in Figure 5.8 because the phonons present in a minuscule space starts vibrating rapidly and the vibrational energy gets converted to the thermal energy as expalained earlier in this Chapter for the X22 case. This explanation is valid for all other values of $\eta > 1.2$ until the effect of hyperbolic heat conduction perishes and classical diffusion takes over.

5.4 Conclusion

In this chapter a complete analysis of thermal wave effect in a dielctric flat plate of miniscule thickness has been demonstrated. At first we examined the X22 case whose solution is given by Eq. (4.34) in the study. Investigating the X22 boundary value problem we observed an existence of a thermal wave, when a sub-micron size dielectric material is heated rapidly in small time. The propagation and reflection of the wave front is well illusrated in this chapter. It was perceived that there is an abrupt jump in temperature at the insulated wall surface and its neighbouring space. The cause of this anomalous rise in surface temperature was elucidated with the aid of phonons vibrating in the lattice in a very small space where their kinetic energy gets converted to thermal energy when they reach their respective excitattion level . Similar explanations were made to justify the rise in temperature for the X12 case when we hold the non-dimensional wall temperature as 1 unit at $x = 0$. In view of the superposition effect in waves, it makes our argument even more stronger to rationalize the observed anomalies.

CHAPTER 6

ESTIMATION OF HEAT FLUX AT THE INTERFACE OF A

TWO-LAYER DIELECTRIC MATERIAL

6.1 Introduction

In this section an attempt has been made to compute the heat flux at the interface of a dielectric substance. The geometry has been shown in Figure 6.1. A bold assumption has been made to simplify the problem by considering the second layer semi-infinite. This assumption was made because in practice the second layer is usually much thicker than the first. An example of this would be CVD decomposition on a silicon substrate. It has been presented widely in the literature that the thickness of the diamond film is around 5 μ in comparison to a 100 μ silicon substrate. These data has encouraged us to consider the second layer semi-infinite. Once again Laplace transform method has been used to estimate the heat flux at the interface considering perfect contact between the two layers. The results for temperature distribution that were derived in previous chapters for different cases have been used with certain necessary modifications.

We start by assuming a prescribed heat flux striking the surface of layer 1 as shown in Figure 6.1. The heat flux is assumed to be a unit pulse striking the surface at $x = 0$ when $t = 0$. Furthermore both the layers have the same initial temperature and it has been assumed to be zero. The problem has been solved by dividing it into three different cases that were discussed in previous chapters. This was done to emphasize on the use of previous results obtained to determine the current results and also to verify the results that were obtained.

6.2 Mathematical Formulation

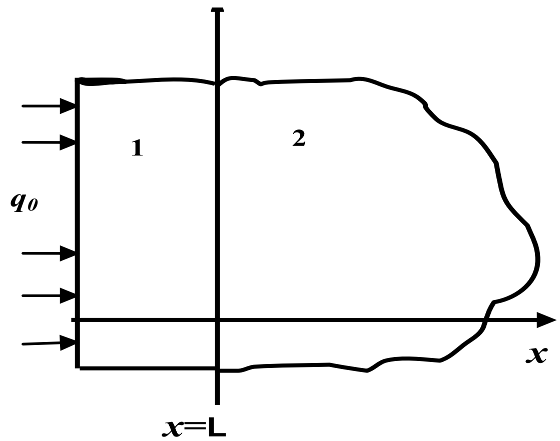

Figure 6.1 Geometry of the problem

By observing the geometry one can comment on the fact that we can compute the heat flux at the interface by dividing the geometry into individual geometries of a plate and a semi-infinite body results of which are derived earlier in previous chapters of this thesis. In this problem we have divided the geometry into three different parts starting with the plate, layer 1, with a unit pulse applied on the surface x = 0 and insulated at x = L. Consequently another plate, layer 1, is considered with desired quantity of heat flux at the interface q at x = L and is insulated at x = 0. Finally the semi-infinite body, layer 2 is considered with the heat flux at interface q at x = L.

Initially we will start with the case accounting for the known quantity of heat flux q_0 on the surface at x = 0 of layer 1. The subscript 1 that will be used later in this section denotes layer 1 and the subscript 1 denotes layer 2. Small modifications are made to reduce the equation to dimensionless form. The dimensionless parameters used in this section are defined as follows,

$\xi \to \frac{x}{L}$ (Dimensionless space)

$\eta \rightarrow \frac{t}{\tau_{q_1}}$ (Dimensionless time)

$\tau_{q_1}{}^* \rightarrow \frac{\alpha_1 \tau_{q_1}}{L^2}$ (Dimensionless lag due to heat flux in layer 1)

$\tau_{q_2}{}^* \rightarrow \frac{\alpha_2 \tau_{q_2}}{L^2}$ (Dimensionless lag due to heat flux in layer 2)

$\theta_1 \rightarrow \frac{k_1(T_1 - T_i)}{q_0 L}$ (Dimensionless temperature in layer 1)

$\theta_2 \rightarrow \frac{k_2(T_2 - T_i)}{q_0 L}$ (Dimensionless temperature in layer 2)

After we have defined all the necessary dimensionless parameters required to solve the problem the following step would be to apply them to the governing equations and equations prevailing the boundary conditions. For layer 1 the following equations are listed below. The governing equation is the same that was used earlier in section 4.2 of Chapter 4. Multiplying both sides of Eq. (4.1) by L^2 we obtain,

$$\frac{\partial^2 T_1}{\partial \xi^2} = \frac{L^2 \ \tau_{q_1}}{\alpha_1 \ \tau_{q_1}} \frac{\partial T_1}{\partial t} + \frac{L^2 \ \tau_{q_1}{}^2}{\alpha_1 \ \tau_{q_1}} \frac{\partial^2 T_1}{\partial t^2} \tag{6.1}$$

$$\frac{\partial^2 T_1}{\partial \xi^2} = \frac{1}{\tau_{q_1}{}^*} \frac{\partial T_1}{\partial \eta} + \frac{1}{\tau_{q_1}{}^*} \frac{\partial^2 T_1}{\partial \eta^2} \tag{6.2}$$

Multiplying both sides of Eq. (6.2) with ($k_1/q_0\, L$) to make it dimensionless in temperature as well because the initial temperature is assumed to be zero.

$$\left(\frac{k_1}{q_0\, L}\right) \frac{\partial^2 T_1}{\partial \xi^2} = \left(\frac{k_1}{q_0\, L}\right) \frac{1}{\tau_{q_1}{}^*} \frac{\partial T_1}{\partial \eta} + \left(\frac{k_1}{q_0\, L}\right) \frac{1}{\tau_{q_1}{}^*} \frac{\partial^2 T_1}{\partial \eta^2} \tag{6.3}$$

$$\frac{\partial^2\theta_1}{\partial\xi^2} = \frac{1}{\tau_{q_1}{}^*}\frac{\partial\theta_1}{\partial\eta} + \frac{1}{\tau_{q_1}{}^*}\frac{\partial^2\theta_1}{\partial\eta^2} \tag{6.4}$$

The Eq. (6.4) is now entirely dimensionless whose Laplace transform is given by,

$$\frac{\partial^2\overline{\theta_1}}{\partial\xi^2} = \left(\frac{s}{\tau_{q_1}{}^*} + \frac{s^2}{\tau_{q_1}{}^*}\right)\overline{\theta_1} \tag{6.5}$$

For simplicity we divide layer 1 in two different sub layers 1a and 1b of same thickness *L*, refer Figure 6.2 and Figure 6.3.

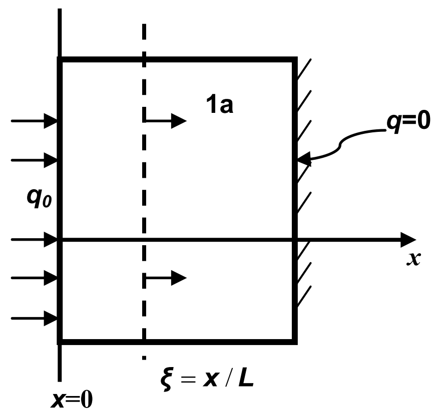

Figure 6.2 Geometry of a finite dielectric body for X22 case.

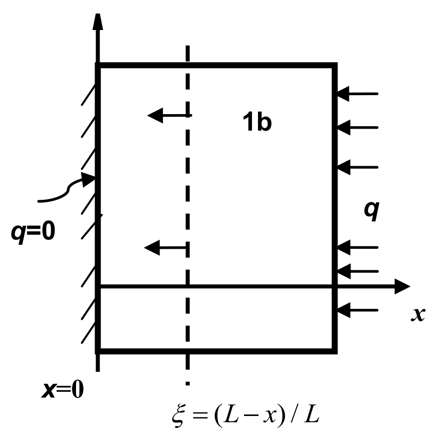

Figure 6.3 Geometry of a finite dielectric body for X22 case where unknown quantity heat flux is at *x* =*L*.

The solution to Eq. (6.5) can be expressed in the same way as Eq. (4.21) but careful consideration has been taken to express the solution for Case 1a and Case 1b pertaining to Figure 6.2 and Figure 6.3 separately. The significant difference in the solution is by replacing ξ with (1-ξ) for the Case 1b. They are represented as follows,

$$\overline{\theta_{1a}} = A\cosh\left[\sqrt{\frac{s+s^2}{\tau_{q_1}{}^*}}\xi\right] + B\sinh\left[\sqrt{\frac{s+s^2}{\tau_{q_1}{}^*}}\xi\right] \tag{6.6}$$

$$\overline{\theta_{1b}} = E\cosh\left[\sqrt{\frac{s+s^2}{\tau_{q_1}{}^*}}\,(1-\xi)\right] + F\sinh\left[\sqrt{\frac{s+s^2}{\tau_{q_1}{}^*}}\,(1-\xi)\right] \tag{6.7}$$

Solving for Case 1a, that is when a unit pulse of heat is applied on the surface at t = 0. The boundary conditions at x = 0 is similar to Eq. (4.8). After making the necessary alterations it becomes,

$$q_0 + \tau_{q_1}\frac{\partial q_0}{\partial t} = -k_1\frac{\partial T_{1a}}{\partial x} \tag{6.8}$$

Multiplying both sides of Eq. (6.8) by L, we acquire,

$$q_0 L + \tau_{q_1} L\frac{\partial q_0}{\partial t} = -k_1 L\frac{\partial T_{1a}}{\partial x} \tag{6.9}$$

$$q_0 L + L\frac{\partial q_0}{\partial \eta} = -k_1\frac{\partial T_{1a}}{\partial \xi} \tag{6.10}$$

Assuming the heat flux as a pulse of unit step we follow the same methodology that was adopted earlier in section 4.2 of Chapter 4, Eq. (4.12 - 4.15) we deduce the following form,

$$1 + \delta(\eta - 0) = -\frac{k_1}{q_0 L}\frac{\partial T_{a1}}{\partial \xi} \tag{6.11}$$

$$1 + \delta(\eta - 0) = -\left.\frac{\partial \theta_{1a}}{\partial \xi}\right|_{\xi = 0} \tag{6.12}$$

By taking the Laplace transform of Eq. (6.12),

$$-\frac{\partial \overline{\theta_{1a}}}{\partial \xi}\bigg|_{\xi=0} = \frac{1}{s}+1 \tag{6.13}$$

Applying Eq. (6.13) to Eq. (6.6) one can acquire the value of the coefficient B in the equation. The following steps lead to determining the value of B.

$$-A\sqrt{\beta(s)}\,(0) - B\sqrt{\beta(s)}\,(1) = \frac{1}{s}+1$$

(6.14)

$$B = \frac{-\left(\frac{1}{s}+1\right)}{\sqrt{\beta(s)}} \tag{6.15}$$

We introduce a new parameter $\beta(s)$ which essentially abbreviates the term $\frac{s+s^2}{\tau_{q_1}^{*}}$. The value of coefficient A can be calculated by using the other boundary condition at $x = L$ where the plate is insulated. Thus we have,

$$-k_1 \frac{\partial T_{1a}}{\partial x}\bigg|_{x=L} = 0 \tag{6.16}$$

$$-\frac{\partial \theta_{1a}}{\partial \xi}\bigg|_{\xi=1} = 0 \tag{6.17}$$

By taking Laplace transform of Eq. (6.17)

$$-\frac{\partial \overline{\theta_{1a}}}{\partial \xi}\bigg|_{\xi=1} = 0$$

Substituting the value of B back in Eq. (6.6) and applying Eq. (6.17) to it would result in obtaining the value of A. The steps are shown as follows,

$$A\cosh\left[\sqrt{\beta(s)}\,\xi\right] - \frac{\left(\frac{1}{s}+1\right)}{\sqrt{\beta(s)}}\sinh\left[\sqrt{\beta(s)}\,\xi\right] = 0 \tag{6.18}$$

$$A = \frac{\left(\frac{1}{s}+1\right)}{\sqrt{\beta(s)}} \coth\left[\sqrt{\beta(s)}\xi\right] \tag{6.19}$$

Thus after obtaining the values of *A* and *B* we substitute them back into Eq. (6.6). The same methodology adopted in Chapter 4 Eq. (4.27- 4.30) is then used to express the equation in an exponential form.

$$\overline{\theta_{1a}} = \frac{\left(\frac{1}{s}+1\right)}{\sqrt{\beta(s)}} \sum_{m=0}^{\infty}\left\{e^{-\left[\sqrt{\beta(s)}(2m+\xi)\right]} + e^{-\left[\sqrt{\beta(s)}\{2(m+1)-\xi\}\right]}\right\} \tag{6.20}$$

Subsequently we calculate the temperature distribution for Case 1b. The geometry of the problem is shown in Figure 6.3. Observing the geometry it is implicit that if do shift of axis then the problem is exactly similar to Case 1a. The prominent difference is the heat flux which in this case is an unknown quantity. The procedure to solve the problem remains the same. The solution to the governing equation is represented as Eq. (6.7) in the study. Hence it is essential to apply the two boundary conditions to calculate the values of the coefficients E and F. At $x = L$ we have heat flux coming in which is given by the equation,

$$q + \tau_{q_1} \frac{\partial q}{\partial t} = -k_1 \frac{\partial T_{1b}}{\partial x} \tag{6.21}$$

$$\frac{q}{q_0} + \frac{1}{q_0}\frac{\partial q}{\partial \eta} = -\frac{\partial \theta_{1b}}{\partial \xi} \tag{6.22}$$

Since q_0 is a known amount of heat flux as assumed earlier in the problem lets specify the value of q_0 to be as unity. Hence after setting $q_0 = 1$ the equation simplifies to the following form,

$$q + \frac{\partial q}{\partial \eta} = -\frac{\partial \theta_{1b}}{\partial \xi} \tag{6.23}$$

The Laplace transform of the above equation is given by,

$$\bar{q} + s\,\bar{q} = -\left.\frac{\partial \overline{\theta_{1b}}}{\partial \xi}\right|_{\xi=1} \tag{6.24}$$

where $\bar{q}$ is the Laplace transform $L\{\ q\ \} = \bar{q}$.

Applying Eq. (6.23) to Eq. (6.7) we can easily find the value of the coefficient F.

$$-E\sqrt{\beta(s)}\ (0) - F\sqrt{\beta(s)}\ (1) = -\left(\bar{q} + s\,\bar{q}\right) \qquad (6.25)$$

$$F = \frac{\left(\bar{q} + s\,\bar{q}\right)}{\sqrt{\beta(s)}} \qquad (6.26)$$

The boundary condition at *x* = 0 is same as the boundary condition at *x* = *L* for the previous Case 1a and thus by similarity we can say that,

$$-\left.\frac{\partial\overline{\theta_{1b}}}{\partial\xi}\right|_{\xi=0} = 0 \qquad (6.27)$$

Using the Eq. (6.27) and Eq. (6.26) we can find the value of E.

$$-E\sinh\left[\sqrt{\beta(s)}\ \right] - \frac{\left(\bar{q} + s\,\bar{q}\right)}{\sqrt{\beta(s)}}\cosh\left[\sqrt{\beta(s)}\ \right] = 0 \qquad (6.30)$$

$$E = -\frac{\left(\bar{q} + s\,\bar{q}\right)}{\sqrt{\beta(s)}}\coth\left[\sqrt{\beta(s)}\ \right] \qquad (6.31)$$

After obtaining the values of *E* and *F* we substitute them back into Eq. (6.7). The same methodology is adopted as in Chapter 4 Eq. (4.27- 4.30) which is then used to express the equation in an exponential form.

$$\overline{\theta_{1b}} = \frac{\left(\bar{q} + s\,\bar{q}\right)}{\sqrt{\beta(s)}}\sum_{m=0}^{\infty}\left\{e^{-\left[\sqrt{\beta(s)}\,(2m+1-\xi)\right]} + e^{-\left[\sqrt{\beta(s)}\,\{2m+1+\xi\}\right]}\right\} \qquad (6.32)$$

Finally we have to consider the semi-infinite body as shown in Figure 6.4. Heat flux of an unknown quantity is applied at the surface x = L. Since at the beginning of the problem we have made the assumption that the two layers are in perfect contact and there is no presence of thermal resistance at the interface.

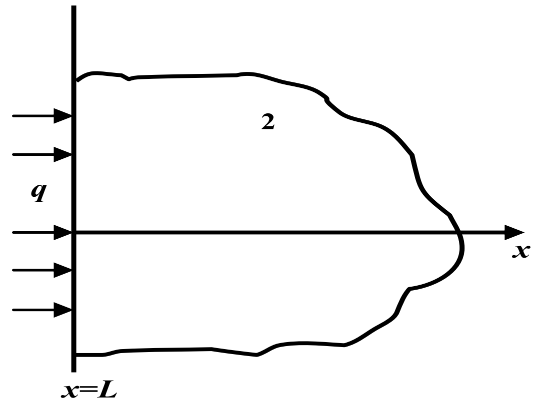

Figure 6.4 A semi-infinite dielectric body with boundary condition X20 at the surface.

Hence the value of this applied unknown quantity of heat flux can be assumed to be q. The formulation of this case is as follows. The governing equation is similar to Eq. (6.1) and is given by,

$$\frac{\partial^2 T_2}{\partial x^2} = \frac{1}{\alpha_2}\frac{\partial T_2}{\partial t} + \frac{\tau_{q_2}}{\alpha_2}\frac{\partial^2 T_2}{\partial t^2} \tag{6.33}$$

The above equation can be made dimensionless in space, time and temperature by undergoing the following steps which are as demonstrated below.

$$L^2 \frac{\partial^2 T_2}{\partial x^2} = \frac{L^2\ \tau_{q_1}}{\alpha_2\ \tau_{q_1}}\frac{\partial T_2}{\partial t} + \left(\frac{L^2}{\alpha_2\ \tau_{q_1}}\right)\left(\frac{\tau_{q_2}}{\tau_{q_1}}\right)\tau_{q_1}^{\ 2}\ \frac{\partial^2 T_2}{\partial t^2} \tag{6.34}$$

$$\frac{\partial^2 T_2}{\partial \xi^2} = \frac{1}{\tau_{q_2}^{\ *}}\frac{\partial T_2}{\partial \eta} + \frac{\varepsilon}{\tau_{q_2}^{\ *}}\frac{\partial^2 T_2}{\partial \eta^2} \tag{6.35}$$

Multiplying both sides of Eq. (6.35) with ($k_2/q_0\,L$) to make it dimensionless in temperature as well because the initial temperature is assumed to be zero. Hence we obtain the subsequent result,

$$\frac{\partial^2\theta_2}{\partial\xi^2} = \frac{1}{\tau_{q_2}{}^*}\frac{\partial\theta_2}{\partial\eta} + \frac{\varepsilon}{\tau_{q_2}{}^*}\frac{\partial^2\theta_2}{\partial\eta^2} \tag{6.36}$$

Taking Laplace transform of Eq. (6.36),

$$\frac{\partial^2\overline{\theta_2}}{\partial\xi^2} = \left(\frac{s}{\tau_{q_2}{}^*} + \frac{s^2\,\varepsilon}{\tau_{q_2}{}^*}\right)\overline{\theta_2} \tag{6.37}$$

Solution of the above differential equation is shown earlier in the study in Chapter 2, section 2.3, Eq. (2.19 - 2.20). Thus we have,

$$\overline{\theta_2} = C_2\ Exp\ [-\sqrt{\lambda(s)}\ (\xi - 1)] \tag{6.38}$$

where $\lambda(s) = \dfrac{s + s^2\,\varepsilon}{\tau_{q_2}{}^*}$ and $\varepsilon = \dfrac{\tau_{q_2}}{\tau_{q_1}}$.

The boundary condition at x = 0 we have heat flux striking the surface of the semi-infinite layer. The value of the heat flux that we are considering here is same as the one considered before for Case 1b. The reason we do so is because it has been stated that there is perfect contact between the two-layers of the dielectric body. The equation is similar to Eq. (6.21) with small variations in existing parameters to denote the layer 2.

$$q + \tau_{q_2}\frac{\partial q}{\partial t} = -k_2\frac{\partial T_2}{\partial x} \tag{6.39}$$

Divide both sides of the equation with q_0 and other ways to make the equation dimensionless, we acquire,

$$\frac{q}{q_0} + \left(\frac{1}{q_0}\right)\left(\frac{\tau_{q_2}}{\tau_{q_2}}\right)\frac{\partial q}{\partial t} = -\left(\frac{k_2\ L}{q_0\ L}\right)\frac{\partial T_2}{\partial x} \tag{6.40}$$

As it has been earlier specified that q_0 = 1, one can further reduce Eq. (6.40) before taking Laplace transform.

$$q+\varepsilon \frac{\partial q}{\partial \eta} = -\left.\frac{\partial \theta_2}{\partial \xi}\right|_{\xi=1} \tag{6.41}$$

$$-\left.\frac{\partial \overline{\theta_2}}{\partial \xi}\right|_{\xi=1} = \bar{q} + \varepsilon\, s\, \bar{q} \tag{6.42}$$

Applying the boundary condition given by Eq. (6.42) to Eq. (6.38) one can calculate value of the coefficient C_2 which is given by,

$$\sqrt{\lambda(s)}\; C_2 = \bar{q}\,(1+\varepsilon\, s) \tag{6.43}$$

$$C_2 = \frac{\bar{q}\,(1+\varepsilon\, s)}{\sqrt{\lambda(s)}} \tag{6.44}$$

Substituting the value of C_2 back in Eq. (6.38) to acquire the following result,

$$\overline{\theta_2} = \frac{\bar{q}\,(1+\varepsilon\, s)}{\sqrt{\lambda(s)}}\, Exp\,[-\sqrt{\lambda(s)}\;(\xi-1)] \tag{6.45}$$

Now by assuming the case of perfect contact between the layers we can equate Eq. (6.20), Eq. (6.32) and Eq. (6.45) by substituting the value of ξ as 1 in each of them. By doing so we obtain the relation,

$$\overline{\theta_{1a}}\,(1,s) + \overline{\theta_{1b}}(1,s) = \overline{\theta_2}(1,s) \tag{6.46}$$

$$\begin{aligned} &\frac{\left(\frac{1}{s}+1\right)}{\sqrt{\beta(s)}} \sum_{m=0}^{\infty}\left\{e^{-\left[\sqrt{\beta(s)}\,(2m+1)\right]} + e^{-\left[\sqrt{\beta(s)}\,\{2(m+1)-1\}\right]}\right\} + \frac{\left(\bar{q}+s\,\bar{q}\right)}{\sqrt{\beta(s)}} \sum_{m=0}^{\infty}\left\{e^{-\left[\sqrt{\beta(s)}\,(2m+1-1)\right]} + e^{-\left[\sqrt{\beta(s)}\,\{2m+1+1\}\right]}\right\} \\ &= \frac{\bar{q}\,(1+\varepsilon\, s)}{\sqrt{\lambda(s)}}\, Exp\,[-\sqrt{\lambda(s)}\;(1-1)] \end{aligned} \tag{6.47}$$

$$2\,\frac{\left(\frac{1}{s}+1\right)}{\sqrt{\beta(s)}} \sum_{m=0}^{\infty}\left\{e^{-\left[\sqrt{\beta(s)}\,(2m+1)\right]}\right\} + \frac{\left(\bar{q}+s\,\bar{q}\right)}{\sqrt{\beta(s)}} \sum_{m=0}^{\infty}\left\{e^{-\left[\sqrt{\beta(s)}\,(2m)\right]} + e^{-\left[\sqrt{\beta(s)}\,\{2(m+1)\}\right]}\right\} = \frac{\bar{q}\,(1+\varepsilon\, s)}{\sqrt{\lambda(s)}} \tag{6.48}$$

Arranging the terms containing $\bar{q}$ on one side we acquire,

$$2\,\frac{\left(\frac{1}{s}+1\right)}{\sqrt{\beta(s)}}\sum_{m=0}^{\infty}\left\{e^{-\left[\sqrt{\beta(s)}\,(2m+1)\right]}\right\} \;=\; \frac{\bar{q}\,(1+\varepsilon\, s)}{\sqrt{\lambda(s)}} \;-\; \frac{\left(\bar{q}+s\,\bar{q}\right)}{\sqrt{\beta(s)}}\sum_{m=0}^{\infty}\left\{e^{-\left[\sqrt{\beta(s)}\,(2m)\right]}+e^{-\left[\sqrt{\beta(s)}\,\{2(m+1)\}\right]}\right\} \tag{6.49}$$

The left side of equation can be solved using standard inverse Laplace transforms but the right side contains the unknown heat flux parameter at the interface which needs to be computed numerically. One of the many approaches in finding the profile for q is that by approximating the variation in the profile with some functions whose Laplace transforms are easily available. For example q could vary either as a second order polynomial or as an exponential function. The numerical analysis of which is not presented in this study.

6.3 Conclusion

In this chapter we have done the complete mathematical formulation to derive Eq. (6.49) which can be used to compute the heat flux at the interface of a two-layer dielectric material. Once again it has been shown how Laplace transforms can be used to solve a complex problem using the existing solutions. The numerical analysis of the heat flux at the interface has been placed as a future work in the study.

CHAPTER 7

FUTURE WORK

It has been well illustrated in this study how classical method of Laplace transform is used to find solutions to semi-infinite, finite and two-layer dielectric bodies. This study can be further can be further extended by numerically estimating the profile for the heat flux at the interface by doing a complete analysis of Eq. (6.49) presented in the study. In addition to that one can compute the Green's function solution of the problem form existing solution that is available in [15]. Another interesting problem would be calculate the temperature profile in a two-layer dielectric material where both the layers are of finite size with both ends insulated and a thin volumetric heat source at the interface. If one can formulate the Green's function solution for the problem defined above then it can be used to find out the temperature solution in the body due to the presence of a volumetric heat source located anywhere within the body. Such problems and many more can be attempted in the future by us and other investigators which will help us explore some other anomalies that exist in heat conduction.

APPENDIX A

MATHEMATICA SUBROUTINE TO COMPUTE THE TEMPERATURE PROFILE FOR A SEMI-INFINITE DIELECTRIC BODY SUBJECTED TO BOUNDARY CONDITION OF FIRST AND SECOND KIND AT x = 0.

1. <u>Semi-Infinite body, X10 problem</u>

```
eta1=4;
Clear[xi];
eta2=7/2;
nt=40;
dx=eta2/nt;
n1=eta1/dx;
n2=eta2/dx;
m=0;
Do[m=m+1;xi[m]=(n-1)*dx;Print[m,"  ",N[xi[m]]],{n,1,n2}];
m=m+1;
xi[m]=eta2-1/10^10;
Print[m,"  ",N[xi[m]]];
Do[m=m+1;xi[m]=eta2+(n-n2)*dx;Print[m,"  ",N[xi[m]]],{n,n2,n1-1}];
m=m+1;
xi[m]=eta1-1/10^10;
Print[m,"  ",N[xi[m]]];
Do[m=m+1;xi[m]=eta1+(n-1)*dx;Print[m,"  ",N[xi[m]]],{n,1,nt+10}];
nst=m

 Clear[x];
f=If[t>x,Exp[-t/2]*BesselI[1,Sqrt[t^2-x^2]/2]/Sqrt[t^2-x^2],0];
eta=eta1;
Do[x=xi[n];
 f0=If[eta>x,Exp[-x/2],0];
 fun=NIntegrate[f,{t,x,eta}];
 ans1[n]=f0+x*fun/2;
 Print[N[x],",  ",N[eta],",  ",N[ans1[n]]],{n,1,nst}]

 Clear[x];
f=If[t>x,Exp[-t/2]*BesselI[1,Sqrt[t^2-x^2]/2]/Sqrt[t^2-x^2],0];
eta=eta2;
Do[x=xi[n];
 f0=If[eta>x,Exp[-x/2],0];
 fun=NIntegrate[f,{t,x,eta}];
 ans2[n]=f0+x*fun/2;Print[N[x],",      ",N[eta],",      ",N[ans1[n]],",      ",N[ans2[n]],",      ",N[ans1[n]-
ans2[n]]],{n,1,nst}]
```

2. <u>Semi-Infinite body, X20 problem</u>

```
eta1=4;
Clear[xi];
eta2=7/2;
```

```
nt=40;
dx=eta2/nt;
n1=eta1/dx;
n2=eta2/dx;
m=0;
Do[m=m+1;xi[m]=(n-1)*dx;Print[m,"  ",N[xi[m]]],{n,1,n2}];
m=m+1;xi[m]=eta2-1/10^10;
Print[m,"  ",N[xi[m]]];
Do[m=m+1;xi[m]=eta2+(n-n2)*dx;Print[m,"  ",N[xi[m]]],{n,n2,n1-1}];
m=m+1;
xi[m]=eta1-1/10^10;
Print[m,"  ",N[xi[m]]];
Do[m=m+1;xi[m]=eta1+(n-1)*dx;Print[m,"  ",N[xi[m]]],{n,1,nt+10}];
nst=m

f=If[t>x,Exp[-t/2]*BesselI[0,Sqrt[t^2-xx^2]/2],0];
eta=eta1;
Do[x=xi[n];
f0=f/.t->eta/.xx->x;
fun=NIntegrate[f/.xx->x,{t,x,eta}];
ans1[n]=f0+fun;Print[N[x],",  ",N[eta],",  ",N[ans1[n]]],{n,1,nst}]

If[t>x,Exp[-t/2]*BesselI[0,Sqrt[t^2-xx^2]/2],0];
eta=eta2;
Do[x=xi[n];
f0=f/.t->eta/.xx->x;
fun=NIntegrate[f/.xx->x,{t,x,eta}];
ans2[n]=f0+fun;
Print[N[x],",  ",N[eta],",  ",N[ans1[n]],",  ",N[ans2[n]],",  ",N[ans1[n]-ans2[n]]],{n,1,nst}]
```

APPENDIX B

MATHEMATICA SUBROUTINE TO COMPUTE THE TEMPERATURE PROFILE FOR A FINITE DIELECTRIC BODY SUBJECTED TO BOUNDARY CONDITION OF FIRST AND SECOND KIND AT x = 0 AND INSULATED BOUNDARY CONDITION AT x = L

1. <u>Plate, X12 problem</u>

```
InvLpTr[a_,kx_,t_]:=(
  ans=If[t>kx,Exp[-a t/2]*BesselI[1,a Sqrt[t^2-kx^2]/2]/Sqrt[t^2-kx^2],0];
  Return[ans])
Print["xi","  ","Time","  Temperature"];
tq=1;
xi=0;
tm=10/10;
np=100;
dtx=1/np;
m=0;
L=1;
aa=1/tq;
Do[fun=0;
sgn=-1;
Do[sgn=-sgn;
k=(xi+2*m*L)*Sqrt[tq];
f0=If[tm>k,Exp[-aa k/2],0];
f1=NIntegrate[InvLpTr[aa,k,t],{t,k,tm}];
fun=fun+(f0+aa*k*f1/2)*sgn;k=(2*L+2*m*L-xi)*Sqrt[tq];
f0=If[tm>k,Exp[-aa k/2],0];
fun=fun+sgn*(f0+aa*k*NIntegrate[InvLpTr[aa,k,t],{t,k,tm}]/2),{m,0,12}];
Print[N[xi],"  ",N[tm],"    ",N[fun],"    ",N[1-fun]];xi=xi+dtx,{j,1,np+1}];
N[fun]
```

2. <u>Plate, X22 problem</u>

```
InvLpTr[a_,kx_,t_]:=(
  ans=If[t>kx,Exp[-a*t/2]*BesselI[0,a Sqrt[t^2-kx^2]/2],0];
  Return[ans])
Print["xi","  ","Time","  Temperature"];
sm=0;
tq=1;
alf=1;
xi=0;
tm=14/10;
np=50;dtx=1/np;
aa=1/tq;
m=0;
L=1;
dtm=6/10;
Do[fun[j]=0;
  Do[k=(xi+2*m*L)*Sqrt[tq/alf];
```

```
   fun[j]=fun[j]+tq*InvLpTr[aa,k,tm]+NIntegrate[InvLpTr[aa,k,t],{t,0,tm}];
   fun[j]=fun[j]-tq*InvLpTr[aa,k,tm-dtm]-NIntegrate[InvLpTr[aa,k,t],{t,0,tm-dtm}];
   k=(2*L+2*m*L-xi)*Sqrt[tq/alf];
   fun[j]=fun[j]+tq*InvLpTr[aa,k,tm]+NIntegrate[InvLpTr[aa,k,t],{t,0,tm}];
fun[j]=fun[j]-tq*InvLpTr[aa,k,tm-dtm]-NIntegrate[InvLpTr[aa,k,t],{t,0,tm-dtm}],{m,0,4}];

sm=sm+N[fun[j]]*dtx;
Print[N[xi],"  ",N[tm],"  ",N[fun[j]]];
xi=xi+dtx,{j,1,np+1}];
plfn=Table[fun[j],{j,1,np+1}];
sm
sm=sm-(N[fun[1]]*dtx+N[fun[np+1]])*dtx/2
sm=sm/dtm

(* Subroutine to calculate the temperature where the jump occurs *)
InvLpTr[a_,kx_,t_]:=(
  ans=If[t>kx,Exp[-a*t/2]*BesselI[0,a Sqrt[t^2-kx^2]/2],0];
  Return[ans])
xi=0.25+1/10^10;
tm=20/10;
dtm=1/4;
tq=1;
alf=1;
aa=1/tq;
m=0;
L=1;
ans1=0;
ans2=0;
Do[k=(xi+2*m*L)*Sqrt[tq/alf];
  ans2=ans2+tq*InvLpTr[aa,k,tm]+NIntegrate[InvLpTr[aa,k,t],{t,0,tm}];
  ans2=ans2-tq*InvLpTr[aa,k,tm-dtm]-NIntegrate[InvLpTr[aa,k,t],{t,0,tm-dtm}];
  k=(2*L+2*m*L-xi)*Sqrt[tq/alf];
  ans1=ans1+tq*InvLpTr[aa,k,tm]+NIntegrate[InvLpTr[aa,k,t],{t,0,tm}];
  ans1=ans1-tq*InvLpTr[aa,k,tm-dtm]-NIntegrate[InvLpTr[aa,k,t],{t,0,tm-dtm}],{m,0,2}];
N[ans2]
N[ans1]
N[ans1+ans2]
```

REFERENCES

[1] Cattaneo, C., A form of heat conduction equation which eliminates the paradox of instantaneous propagation, Compte Rendus Vol. 247 (1958) 431-433.

[2] Vernotte, P., Some possible complications in the phenomena of thermal conduction, Compte Rendus Vol. 252 (1961) 2190-2191.

[3] Tien, C. L. and Lienhardt, J. H., Statistical Thermodynamics, McGraw-Hill, New York, 1979.

[4] Qui, T. Q. and Tien, C. L., Short-pulse laser heating on metals, International Journal of Heat and Mass Transfer, Vol. 35, (1992) 719-726.

[5] Qui, T. Q. and Tien, C. L., Heat transfer mechanisms during short-pulse laser heating on metals, ASME Journal of Heat Transfer, Vol. 115, (1993) 835-841.

[6] Joseph, D. D. and Preziosi, L., Heat waves, Rev. Mod. Phys. Vol. 61, (1989) 41-73.

[7] Tzou, Da Yu, The generalized lagging response in small-scale and high-rate heating, Int. J. of Heat and Mass Transfer, Vol. 38 (1995) 3231-3240.

[8] Ho, J-R, Kuo, C-P, Jiaung, W-S, Study of heat transfer in multilayered structure within the framework of dual-phase-lag heat conduction model using lattice Boltzmann method, Int. J. of Heat and Mass Transfer, Vol. 46, (2003) 55-69.

[9] Kittel, C., Introduction to Solid State Physics, Sixth Edition, John Wiley and Sons, New York, 1986, pp. 139-141.

[10] Ozisik, M. N. and Tzou, D. Y., On the wave theory in heat conduction, ASME Journal of Heat Transfer, Vol. 116, (1994) 526-535.

[11] Frankel, J. I., Vick, B., and Ozisik, M. N., Flux formulation of hyperbolic heat conduction, Journal of Applied Physics, Vol. 58, (1985) 3340-3345.

[12] Hays-Stang, K. J. and Haji-Sheikh, A., A unified solution for heat conduction in thin films, International Journal of Heat and mass Transfer, Vol. 42, (1999) 455-465.

[13] Tzou, D. K., Macro- to Microscale Heat Transfer, Taylor and Francis, New York, 1997.

[14] Haji-Sheikh, A., Minkowycz, W. J., and Sparrow, E. M., Certain anomalies in the analysis of hyperbolic heat conduction, ASME Journal of Heat Transfer, Vol. 124, (2002) 307-319.

[15] Haji-Sheikh, A. and Beck, J. V., Green's function solution for thermal wave equation in finite bodies, International Journal of Heat and Mass Transfer, Vol, 37, (1994) 2615-2626.

[16] Beck, J. V., Cole, K. D. Haji-Sheikh, A., and Litkouhi, B, Heat Conduction Using Green's Functions, Hemisphere Publishing Corp., Washington, D. C., 1992.

[17] Baumeister, K. J. and Hamill, T. D., Hyperbolic heat conduction equation—A solution for the semi-infinite problem, ASME Journal of Heat Transfer, Vol. 91, (1969) 543-548.

[18] Churchill, R. V., *Operational Mathematics*, McGraw-Hill, New York, 1958.

[19] Ozisik, M.N. and Vick, B., Propagation and reflection of thermal waves in finite medium, International Journal of Heat and Mass Transfer, Vol. 27, No. 10, (1984), 1845-1854.

[20] Tzou, D.Y., K.S. Chiu, Temperature dependent thermal lagging in ultrafast laser heating, International Journal of Heat and Mass Transfer, 44(2001), 1725-1734.

[21] Mitra, K., Kumar, S., Vedavarz, A., Moallemi, M.K., Experimental Evidence of Hyperbolic Heat Conduction in Processed Meat, ASME Journal of Heat Transfer, Vol. 117, August 1995, 568-573.

[22] A.F. Khadwari, M.A. Al-Nimr, M. Hammad, Thermal Behavior of Perfect and Imperfect Contact Composite Slabs Under the Effect of the Hyperbolic Heat Conduction Model., International Journal of Thermophysics, vol. 23, No. 2, March 2002.

[23] Lor, Whey-Bin, Chu Hsin-Sen, Effect of Interface thermal resistance on heat transfer in a composite medium using the thermal wave model, International Journal of Heat and Mass Transfer, 43 (2000), 653-663.

[24] Li, J., Cheng, P., Peterson, G.P., Xu, J.Z., Rapid Transient Heat Conduction in Multilayer Materials With Pulsed Heating Boundary, Numerical Heat Transfer, Part A, Taylor & Francis Inc., 47, 2005, 633-652.

[25] Kronberg A. E., Benneker, A.H., Westerterp, K.R., Notes on wave theory in heat conduction: a new boundary condition, International Journal of Heat and Mass Transfer, Vol. 41, No.1, 1998, 127-137.

[26] Tang, D.W., Araki, N., Wavy, wavylike, diffusive thermal responses of finite rigid slabs to high-speed heating of laser-pulses, International Journal of Heat and Mass Transfer, 42, 1999, 855-860.

BIOGRAPHICAL INFORMATION

Daipayan Sarkar is pursuing his Master of Science in Mechanical Engineering at University of Texas at Arlington. He obtained his Bachelors of Engineering in Mechanical Engineering from Fr. C. Rodrigues Institute of Technology, Vashi, affiliated to University of Mumbai, India. He has maintained a good overall academic record in his time in University of Texas at Arlington as a graduate student. His area of interest is Condensed Matter Physics, High Temperature Physics, Macro and Micro-scale heat transfer, Convective heat transfer in Porous Media, Finite Element methods in heat transfer and fluid flow, 3D Integrated Circuit Packaging, Computational Fluid Dynamics, Numerical Analysis of different functions. After graduating from University of Texas at Arlington he plans to continue his learning process by pursuing his Doctoral studies here in the United States. Apart from academics his other interests are soccer, experiencing different cuisines and travelling to different places and understanding and appreciating their culture.